# Pushing the limits of electronic donation for *cis*-chelating ligands *via* an alliance of phosphonium ylide and anionic abnormal NHC

Mustapha El Kadiri,[a,b] Abdelhaq Cherradi,[a] Oleg A. Filippov,[c]* Carine Duhayon,[a] Vincent César,[a] Elena S. Shubina,[c] Mohammed Lahcini,[b,d]* Dmitry A. Valyaev[a]* and Yves Canac[a]*

[a] LCC–CNRS, Université de Toulouse, CNRS, 205 route de Narbonne 31077 Toulouse Cedex 4, France.
E-mail: dmitry.valyaev@lcc-toulouse.fr, yves.canac@lcc-toulouse.fr
[b] IMED-Lab, Faculty of Sciences and Techniques, Cadi Ayyad University, Avenue Abdelkrim Elkhattabi, B.P. 549, 40000 Marrakech, Morocco.
E-mail: m.lahcini@uca.ac.ma
[c] A. N. Nesmeyanov Institute of Organoelement Compounds (INEOS), Russian Academy of Sciences, 28/1 Vavilov str., GSP-1, B-334, Moscow, 119334, Russia.
E-mail: h-bond@ineos.ac.ru
[d] Mohammed VI Polytechnic University, Lot 660, Hay Moulay Rachid, Ben Guerir 43150, Morocco.

## Electronic Supplementary Information

## Table of contents

## General information

All manipulations were performed under an inert atmosphere of dry nitrogen using standard vacuum line and Schlenk techniques. Glassware was dried at 120°C in an oven for at least three hours. Pentane $Et_2O$, toluene and $CH_2Cl_2$ were dried using an Innovative Technology solvent purification system. Acetonitrile was dried using a MBraun SPS column. Tetrahydrofuran was dried and distilled from sodium/benzophenone mixture and stored over Na/K alloy under inert atmosphere. Chlorobenzene was distilled over $CaH_2$ and stored under an inert atmosphere. Chromatographic purification was carried out on silica gel ($SiO_2$, 63−200 µm) using solvents deoxygenated by nitrogen bubbling. Solution IR spectra were recorded in 0.1 mm $CaF_2$ cells using a Perkin Elmer Frontier FT-IR spectrometer and given in $cm^{-1}$. $^1H$, $^{31}P$, and $^{13}C$ NMR spectra were obtained on Bruker AV400HD, AV400NEO or NEO600 spectrometers. NMR chemical shifts $\delta$ are in ppm, with positive values to high frequency relative to the tetramethylsilane reference for $^1H$ and $^{13}C$, and to 85% $H_3PO_4$ for $^{31}P$. If necessary, additional information on the carbon signal attribution was obtained using $^{13}C\{^1H,^{31}P\}$, DEPT and $^1H–^{13}C$ HSQC experiments. High-resolution MS spectra (ESI mode) were performed by the mass spectrometry service of the "Institut de Chimie de Toulouse" using using a Xevo G2 QTof (Waters) spectrometer. Elemental analyses were performed by the elemental analysis service of the LCC with a Perkin Elmer 2400 series II analyzer. Complex **1** was prepared according to previously described procedure.[1] All other reagent-grade chemicals purchased from commercial sources were used as received.

## Synthesis and characterization of NHC complexes

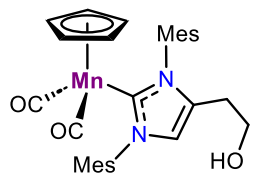

**2**

**Synthesis of complex 2.** To a yellow solution of complex $[Cp(CO)_2Mn(IMes)]$ (**1**) (2.88 g, 6.0 mmol) in dry THF (50 mL), *n*BuLi (4.5 mL of 1.6 M in hexanes, 7.2 mmol, 1.2 equiv.) was added dropwise at RT. The resulting orange solution was stirred for 15 min and IR spectrum of the reaction aliquot showed the quantitative formation of the intermediate $[Cp(CO)_2Mn(IMesLi)]$ ($\nu_{CO}$ 1900, 1831 $cm^{-1}$). Then, the reaction mixture was cooled to −40°C and ethylene oxide (4.8 mL of 2.5 M in THF, 12 mmol, 2.0 equiv.) was added dropwise. The resulting solution was warmed up to RT for 2 h, quenched with degassed water (0.5 mL) and evaporated under vacuum. The residue was dissolved in dry DCM (30 mL) and the solution was filtered over Celite to remove LiOH and again evaporated under vacuum. The product was purified by column chromatography on silica (3×20 cm) under nitrogen atmosphere. Some unreacted starting material **1** was eluted first with pure toluene as a yellow zone followed by the deep-orange band of the product eluted using toluene/THF 5:2 mixture. The eluate was evaporated under vacuum and the resulting oily solid was triturated with degassed hexane (50 mL) and dried to afford complex **2** as a yellow powder (2.98 g, 95%).

$^1H$ NMR (400.1 MHz, $C_6D_6$, 25°C): δ 6.88 (s, 4H, C*H*$_{Mes}$), 6.26 (s, 1H, C*H*$_{Im\text{-}5}$), 4.02 (s, 5H, Cp), 3.19 (t, $^3J_{HH}$ = 6.0 Hz, 2H, $ImCH_2CH_2OH$), 2.19 (s, 3H, C*H*$_{3Mes}$), 2.18 (s, 3H, C*H*$_{3Mes}$), 2.11 (s, 6H, C*H*$_{3Mes}$), 2.03 (s, 6H, C*H*$_{3Mes}$), 1.97 (t, $^3J_{HH}$ = 6.0 Hz, 2H, $ImCH_2CH_2OH$), 0.50 ppm (br. s, 1H, $ImCH_2CH_2OH$); $^{13}C\{^1H\}$ NMR (100.6 MHz, $C_6D_6$, 25°C): δ 234.6 (s, Mn−*C*O), 204.0 (s, Mn−*C*N$_2$), 138.7, 138.4, 136.8, 136.3, 136.2 (s, *C*$_{Mes}$), 133.3 (s, *C*$_{Im\text{-}4}$), 129.7, 129.4 (s, *C*H$_{Mes}$), 121.3 (s, *C*H$_{Im\text{-}5}$), 81.6 (s, Cp), 59.9 (s, $ImCH_2CH_2OH$), 28.6 (s, $ImCH_2CH_2OH$), 21.2, 21.1, 18.6, 18.5 ppm (s, *C*H$_{3Mes}$). IR (THF): $\nu_{CO}$ 1913, 1845 $cm^{-1}$. HRMS ($ESI^+$): calcd for $C_{30}H_{33}MnN_2O_3$, 524.1872; found, 524.1877 ($\varepsilon_r$ = 1.0 ppm). Elemental analysis for $C_{30}H_{33}MnN_2O_3$: calcd, C 68.69, H 6.34, N 5.34; found, C 69.05, H 6.54, N 5.20.

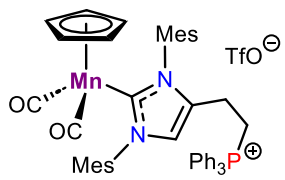

[**3a**](OTf)

**Synthesis of complex [3a](OTf).** To a solution of complex **2** (525 mg, 1.0 mmol) in THF (15 mL) *n*BuLi (0.7 mL of 1.6 M in hexanes, 1.1 mmol, 1.1 equiv.) was added dropwise at RT and the resulting mixture was stirred for 20 min and evaporated under vacuum. The residue was dissolved in dry chlorobenzene (15 mL), the resulting solution was cooled to −40°C and $Tf_2O$ (185 µL, 1.1 mmol, 1.1 equiv.) was added dropwise and the reaction mixture was allowed to warm up to RT for *ca.* 1 h. After addition of $PPh_3$ (787 mg, 3.0 mmol, 3.0 equiv.), the solution was heated at 80°C for 16 h and then all volatiles were evaporated under vacuum. The resulting brown solid was washed with $Et_2O$ (3×20 mL), dissolved in $CH_2Cl_2$ (10 mL), filtered over Celite and the product was precipitated by addition of ether (15 mL). The supernatant was removed by decantation to afford after drying under vacuum complex [**3a**](OTf) (690 mg, 75%) as a yellow powder. Single crystals suitable for X-ray diffraction study were obtained by vapor diffusion of ether into the solution of complex [**3a**](OTf) in toluene.

$^1$H NMR (400.1 MHz, $CD_3CN$, 25°C): δ 7.89−7.84 (m, 3H, C*H*$_{Ph}$), 7.69−7.64 (m, 6H, C*H*$_{Ph}$), 7.56−7.51 (m, 6H, C*H*$_{Ph}$), 7.05 (br. s, 3H, C*H*$_{Im\text{-}5}$ + C*H*$_{Mes}$), 7.00 (s, 2H, C*H*$_{Mes}$), 3.96 (s, 5H, Cp), 3.26−3.18 (m, 2H, PC*H*$_2$CH$_2$Im), 2.39−2.30 (m overlapped with two s signals, 8H, PCH$_2$C*H*$_2$Im + C*H*$_{3Mes}$), 2.07 (s, 6H, C*H*$_{3Mes}$), 1.92 (s, 6H, C*H*$_{3Mes}$); $^{31}$P{$^1$H} NMR (162.0 MHz, $CD_3CN$, 25°C): δ 22.7 ppm (s); $^{13}$C{$^1$H} NMR (100.6 MHz, $CD_3CN$, 25°C): δ 235.3 (Mn−*C*O), 203.9 (Mn−*C*N$_2$), 139.9, 139.5, 139.0, 137.4, 137.1 (s, *C*$_{Mes}$), 136.4 (d, $J_{CP}$ = 3.0 Hz, C*H*$_{Ph}$), 136.1 (s, *C*$_{Mes}$), 134.5 (d, $J_{CP}$ = 11.1 Hz, *C*H$_{Ph}$), 133.7 (d, $J_{CP}$ = 21.1 Hz, *C*$_{ipso\ Ph}$), 131.4 (d, $J_{CP}$ = 13.1 Hz, *C*H$_{Ph}$), 130.4, 129.8 (s, C*H*$_{Mes}$), 124.1 (s, C*H*$_{Im\text{-}5}$), 122.2 (q, $^1J_{CF}$ = 319.9 Hz, *C*F$_3$SO$_3$), 82.4 (s, Cp), 21.4 (d, $^1J_{CP}$ = 51.3 Hz, P*C*H$_2$CH$_2$Im), 21.3, 21.2 (s, *C*H$_{3Mes}$), 18.8 (brs, PCH$_2$*C*H$_2$Im), 18.7, 18.6 (s, *C*H$_{3Mes}$). IR (THF): $\nu_{CO}$ 1912, 1845 cm$^{-1}$. MS (ESI$^+$): *m/z* 769.3 [M–OTf]$^+$; HRMS (ESI$^+$): calcd for $C_{48}H_{47}MnN_2O_2P$, 769.2756; found, 769.2746 ($\varepsilon_r$ = 1.3 ppm). Elemental analysis for $C_{49}H_{47}F_3MnN_2O_5PS\times0.3CH_2Cl_2$: calcd, C 62.70, H 5.08, N 2.97; found, C 62.61, H 5.64, N 3.06.

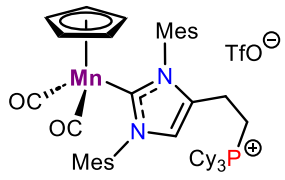

[**3b**](OTf)

**Synthesis of complex [3b](OTf).** To a solution of complex **2** (525 mg, 1.0 mmol) in THF (15 mL) *n*BuLi (0.7 mL of 1.6 M in hexanes, 1.1 mmol, 1.1 equiv.) was added dropwise at RT and the resulting mixture was stirred for 20 min and evaporated under vacuum. The residue was dissolved in dry chlorobenzene (15 mL), the resulting solution was cooled to −40°C and $Tf_2O$ (185 µL, 1.1 mmol, 1.1 equiv.) was added dropwise and the reaction mixture was allowed to warm up to RT for *ca.* 1 h. After addition of $PCy_3$ (420 mg, 1.5 mmol, 1.5 equiv.), the solution was heated at 60°C for 16 hours and then all volatiles were evaporated under vacuum. The resulting brown solid was washed with $Et_2O$ (3×20 mL), dissolved in $CH_2Cl_2$ (10 mL), filtered over Celite and the product was precipitated by addition of ether (15 mL). The supernatant was removed by decantation to afford after drying under vacuum complex [**3b**](OTf) (750 mg, 80%) as a yellow powder. Single crystals suitable for X-ray diffraction study were obtained by the crystallization in toluene/ethanol mixture at RT.

$^1$H NMR (400.1 MHz, $CD_3CN$, 25°C): δ 7.13 (s, 2H, C*H*$_{Mes}$), 7.09 (s, 1H, C*H*$_{Im\text{-}5}$), 7.06 (s, 2H, C*H*$_{Mes}$), 3.98 (s, 5H, Cp), 2.45−2.25 (m with two overlapped singlets, 11H, PC*H*$_2$CH$_2$Im + C*H*$_{Cy}$ + C*H*$_{3Mes}$), 2.18−2.14 (m, 2H, PCH$_2$C*H*$_2$Im), 2.09 (s, 6H, C*H*$_{3Mes}$), 2.07 (s, 6H, C*H*$_{3Mes}$), 1.85−1.65 (m, 15H, C*H*$_{2Cy}$), 1.40−1.20 ppm (m, 15H, C*H*$_{2Cy}$); $^{31}$P{$^1$H} NMR (162.0 MHz, $CD_3CN$, 25°C): δ 31.3 ppm (s); $^{13}$C{$^1$H} NMR (100.6 MHz, $CD_3CN$, 25°C): δ 235.3 (Mn−*C*O), 203.9 (Mn−*C*N$_2$), 140.1, 139.5, 139.0, 137.6, 137.0, 136.3 (s, *C*$_{Mes}$), 134.0 (d, $^3J_{CP}$ = 17.1 Hz, *C*$_{Im\text{-}4}$), 130.6, 129.8 (s, *C*H$_{Mes}$), 124.3 (s, *C*H$_{Im\text{-}5}$), 122.2

(q, $^1J_{CF}$ = 320.9 Hz, $CF_3SO_3$), 82.4 (s, Cp), 30.0 (d, $J_{CP}$ = 40.2 Hz, $CH_{Cy}$), 27.3 (d, $J_{CP}$ = 4.0 Hz, $CH_{2Cy}$), 27.0 (d, $J_{CP}$ = 12.1 Hz, $CH_{2Cy}$), 25.9 (s, $CH_{2Cy}$), 21.3, 21.2 (s, $CH_{3Mes}$), 19.0 (d, $^2J_{CP}$ = 3.0 Hz, $PCH_2CH_2Im$), 18.9, 18.7 (s, $CH_{3Mes}$), 15.7 (d, $^1J_{CP}$ = 41.2 Hz, $PCH_2CH_2Im$). IR (THF): $\nu_{CO}$ 1912, 1845 $cm^{-1}$. MS ($ESI^+$): *m/z* 787.4 $[M–OTf]^+$; HRMS ($ESI^+$): calcd for $C_{48}H_{65}MnN_2O_2P$, 787.4164; found, 787.4161 ($\varepsilon_r$ = 0.4 ppm). Elemental analysis for $C_{49}H_{65}F_3MnN_2O_5PS$: calcd, C 62.81, H 6.99, N 2.99; found, C 62.02, H 7.21, N 2.81.

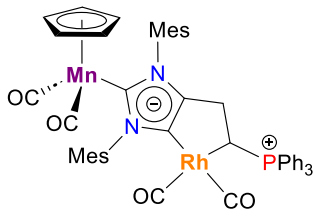

**5a**

**Synthesis of complex 5a**. To a yellow solution of complex [**3a**](OTf) (80 mg, 0.09 mmol) in dry THF (3 mL), *n*BuLi (140 µL of 1.6 M in hexanes, 2.5 equiv.) was added dropwise at RT. The resulting deep-orange solution was stirred for 15 min and IR spectrum of the reaction aliquot showed the formation of complex **4a** as a sole product ($\nu_{CO}$ 1899, 1829 $cm^{-1}$). After evaporation of THF under vacuum, the residue was redissolved in toluene (4 mL), cooled to −40°C and $[Rh(CO)_2Cl]_2$ (22 mg, 0.054 mmol, 0.6 equiv.) was added. The reaction mixture was warmed up to RT for 1 h to afford complex **5a** as a major product according to IR analysis ($\nu_{CO}$ 2036, 1968, 1906, 1838 $cm^{-1}$). Toluene was evaporated under vacuum and the residue was extracted with $Et_2O$ (3×10 mL) under sonication. Combined extracts were filtered over Celite and evaporated under vacuum to afford complex **5a** (73 mg, 88%) as orange solid. Single crystals suitable for X-ray diffraction analysis were obtained from the solution of complex **5a** in THF/toluene/pentane mixture at −20°C. Due to a gradual isomerization of complex **5a** into **6a** in solution, few signals from aromatic region cannot be reliably distinguished.

$^1H$ NMR (400.1 MHz, $C_6D_6$, 25°C): δ 7.48–7.43 (m, 6H, $CH_{Ph}$), 7.18 (s, 1H, $CH_{Mes}$), 7.06 (s, 1H, $CH_{Mes}$), 7.00–6.95 (m, 3H, $CH_{Ph}$), 6.89 (s, 1H, $CH_{Mes}$), 6.88–6.81 (m, 6H, $CH_{Ph}$), 6.78 (s, 1H, $CH_{Mes}$), 4.15 (s, 5H, Cp), 3.07–2.93 (m, 2H, $PCHCH_2Im$), 2.60 (s, 3H, $CH_{3Mes}$), 2.57–2.51 (m, 1H, $PCHCH_2Im$), 2.47 (s, 3H, $CH_{3Mes}$), 2.32 (s, 3H, $CH_{3Mes}$), 2.29 (s, 3H, $CH_{3Mes}$), 2.10 (s, 3H, $CH_{3Mes}$), 1.55 ppm (s, 3H, $CH_{3Mes}$); $^{31}P\{^1H\}$ NMR (162.0 MHz, $C_6D_6$, 25°C): δ 41.2 ppm (s); $^{13}C\{^1H\}$ NMR (100.6 MHz, $C_6D_6$, 25°C): δ 235.4, 235.2 (s, Mn−*C*O), 199.9 (s, Mn−$CN_2$), 191.9 (d, $^1J_{CRh}$ = 50.3 Hz, Rh−*C*O), 187.5 (d, $^1J_{CRh}$ = 63.9 Hz, Rh−*C*O), 162.7 (d, $^1J_{CRh}$ = 42.5 Hz, Rh−$C_{Im\text{-}5}$), 152.2 (dd, $J_{CP}$ = 11.5 Hz, $J_{CRh}$ = 5.4 Hz, $C_{Im\text{-}4}$), 143.4, 138.9, 137.6, 137.5, 137.4, 136.8, 136.2, 136.1 (s, $C_{Mes}$), 134.0 (d, $J_{PC}$ = 9.2 Hz, $CH_{Ph}$), 133.0 (d, $J_{PC}$ = 2.8 Hz, $CH_{Ph}$), 129.5 (d, $J_{PC}$ = 2.8 Hz, $CH_{Ph}$), 129.35, 129.3, 129.15, 129.1 (s, $CH_{Mes}$), 129.0 (d, $J_{PC}$ = 11.5 Hz, $CH_{Ph}$), 128.2, 128.0 (s, $CH_{Ph}$), 125.6 (d, $^1J_{CP}$ = 83.2 Hz, $C_{ipso\ Ph}$), 81.9 (s, Cp), 28.7 (s, $CH_2$, $PCHCH_2Im$), 21.4, 21.2, 20.0, 19.6, 18.8, 17.9 (s, $CH_{3Mes}$), 13.9 ppm (dd, $^1J_{CRh}$ = 27.5 Hz, $^1J_{CP}$ = 25.5 Hz, $PCHCH_2Im$). HRMS ($ESI^+$): calcd for $C_{50}H_{45}MnN_2O_4PRh$, 926.1552; found, 926.1576 ($\varepsilon_r$ = 2.6 ppm). IR (THF): $\nu_{CO}$ 2035, 1966, 1906, 1838 $cm^{-1}$. IR (toluene): $\nu_{CO}$ 2036, 1968, 1906, 1838 $cm^{-1}$.

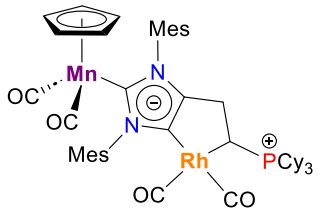

**5b**

**Synthesis of complex 5b.** To a yellow solution of complex [**3b**](OTf) (85 mg, 0.09 mmol) in dry THF (4 mL), *n*BuLi (140 µL of 1.6 M in hexanes, 2.5 equiv.) was added dropwise at RT. The resulting deep-orange solution was stirred for 15 min and IR spectrum of the reaction aliquot showed the formation of complex **4b** as a sole product ($\nu_{CO}$ 1898, 1828 $cm^{-1}$). After evaporation of THF under vacuum, the residue was redissolved in toluene (4 mL), cooled to −40°C and $[Rh(CO)_2Cl]_2$ (22 mg, 0.054 mmol, 0.6 equiv.) was added. The reaction mixture was warmed up to RT for 1 h to afford complex **5b** as a major product according to IR analysis ($\nu_{CO}$ 2033, 1953, 1907, 1839 $cm^{-1}$). Toluene was evaporated

under vacuum and the residue was extracted with $Et_2O$ (3×10 mL) under sonication. Combined extracts were filtered over Celite and evaporated under vacuum to afford complex **5b** (77 mg, 90%) as red-orange solid.

$^1$H NMR (600.2 MHz, $C_6D_6$, 25°C): δ 7.12 (s, 1H, C*H*$_{Mes}$), 7.09 (s, 1H, C*H*$_{Mes}$), 7.00 (s, 1*H*, CH$_{Mes}$), 6.94 (s, 1H, C*H*$_{Mes}$), 4.20 (s, 5H, Cp), 2.72–2.66 (m, 1H, PCHC*H*$_2$Im), 2.54 (s, 3H, C*H*$_{3Mes}$), 2.52 (s, 3H, C*H*$_{3Mes}$), 2.49–2.45 (m, 1H, PCHC*H*$_2$Im), 2.32 (s, 3H, C*H*$_{3Mes}$), 2.29 (s, 3H, C*H*$_{3Mes}$), 2.28 (s, 3H, C*H*$_{3Mes}$), 2.18 (s, 3H, C*H*$_{3Mes}$), 2.15–2.10 (m, 1H, PC*H*CH$_2$Im), 1.98–1.92 (m, 3H, C*H*$_{Cy}$), 1.63–1.56 (m, 3H, C*H*$_{2Cy}$), 1.53−1.34 (m, 15H, C*H*$_{2Cy}$), 1.24–1.15 (m, 3H, C*H*$_{2Cy}$), 1.00–0.87 (m, 6H, C*H*$_{2Cy}$), 0.85−0.76 ppm (m, 3H, C*H*$_{2Cy}$); $^{31}$P{$^1$H} NMR (243.0 MHz, $C_6D_6$, 25°C): δ 43.6 ppm (s); $^{13}$C{$^1$H} NMR (150.9 MHz, $C_6D_6$, 25°C): δ 235.6, 235.2 (s, Mn−*C*O), 200.5 (s, Mn−*C*N$_2$), 195.2 (d, $^1J_{CRh}$ = 54.3 Hz, Rh−*C*O), 187.7 (d, $^1J_{CRh}$ = 62.2 Hz, Mn−*C*O), 162.2 (d, $^1J_{CRh}$ = 42.7 Hz, Rh−*C*$_{Im-5}$), 152.1 (dd, $^3J_{CP}$ = 13.5 Hz, $^2J_{CRh}$ = 6.0 Hz, *C*$_{Im-4}$), 143.4, 139.1, 137.7, 137.6, 137.5, 136.7, 136.5, 135.9 (s, *C*$_{Mes}$), 129.7, 129.6, 129.3, 129.2 (s, C*H*$_{Mes}$), 81.9 (s, Cp), 32.5 (d, $^1J_{CP}$ = 42.3 Hz, *C*H$_{Cy}$), 27.9 (s, PCH*C*H$_2$Im), 27.6 (s, *C*H$_{2Cy}$), 27.2 (d, $J_{CP}$ = 10.6 Hz, *C*H$_{2Cy}$), 27.0 (s, *C*H$_{2Cy}$), 26.6 (d, $J_{CP}$ = 10.6 Hz, *C*H$_{2Cy}$), 25.8 (s, *C*H$_{2Cy}$), 21.4, 21.3, 20.0, 19.7, 18.8, 18.7 (s, *C*H$_{3Mes}$), 6.4 (dd, $^1J_{CRh}$ = 25.7 Hz, $^1J_{CP}$ = 19.6 Hz, P*C*HCH$_2$Im). MS (ESI$^+$): *m/z* 944.3 [M]$^+$; HRMS (ESI$^+$): calcd for $C_{50}H_{63}MnN_2O_4PRh$, 944.2961; found, 944.2971 ($\varepsilon_r$ = 1.1 ppm). IR (THF): $\nu_{CO}$ 2030, 1952, 1906, 1838 cm$^{-1}$. IR (toluene): $\nu_{CO}$ 2033, 1953, 1907, 1839 cm$^{-1}$.

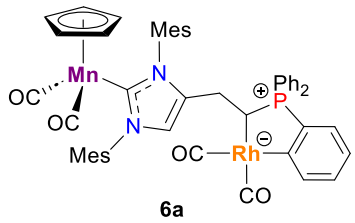

**6a**

**Synthesis of complex 6a.** The solution of complex **5a** (80 mg, 0.08 mmol) in toluene (5 mL) was heated at 50°C until the complete formation of **6a** observed by IR spectroscopy (*ca.* 20 h). The solvent was evaporated under vacuum and the residue was purified by chromatography on silica column (10×1 cm) under nitrogen atmosphere. A yellow-orange zone of the product was eluted with toluene to afford after solvent evaporation complex **6a** (68 mg, 95%) as an orange solid.

$^1$H NMR (400.1 MHz, $C_6D_6$, 25°C): δ 8.36 (d, $J_{HH}$ = 8.0 Hz, 1H, C*H*$_{Ph}$), 7.30−7.24 (m, 2H, C*H*$_{Ph}$), 7.14−7.09 (m, 1H, C*H*$_{Ph}$), 7.07−6.99 (m, 3H, C*H*$_{Ph}$), 6.97−6.84 (m, 8H, C*H*$_{Ph}$ + C*H*$_{Mes}$ + C*H*$_{Im-5}$), 6.81−6.76 (m, 2H, C*H*$_{Ph}$), 6.75 (s, 1H, C*H*$_{Mes}$), 6.71 (s, 1H, C*H*$_{Mes}$), 4.04 (s, 5H, Cp), 2.78−2.72 (m, 2H, PCHC*H*$_2$Im), 2.46−2.36 (m, 1H, PC*H*CH$_2$Im), 2.28 (s, 3H, C*H*$_{3Mes}$), 2.22 (s, 3H, C*H*$_{3Mes}$), 2.19 (s, 3H, C*H*$_{3Mes}$), 2.12 (s, 3H, C*H*$_{3Mes}$), 2.04 (s, 3H, C*H*$_{3Mes}$), 2.035 ppm (s, 3H, C*H*$_{3Mes}$); $^{31}$P{$^1$H} NMR (162.0 MHz, $C_6D_6$, 25°C): δ 27.8 ppm (d, $^2J_{PRh}$ = 2.4 Hz); $^{13}$C{$^1$H} NMR (100.6 MHz, $C_6D_6$, 25°C): δ 234.7, 234.6 (s, Mn−*C*O), 204.5 (s, Mn−*C*N$_2$), 194.0 (dd, $^1J_{CRh}$ = 54.1 Hz, $^3J_{CP}$ = 7.2 Hz, Rh−*C*O), 191.1 (dd, $^1J_{CRh}$ = 64.7 Hz, $^3J_{CP}$ = 4.4 Hz, Rh−*C*O), 181.6 (t, $^1J_{CRh}$ = $^2J_{CP}$ = 33.7 Hz, Rh−*C*$_{Ph}$), 143.4 (dd, $^3J_{CP}$ = 19.3 Hz, $^3J_{CRh}$ = 2.2 Hz, *C*H$_{Ph}$), 138.8, 138.4, 138.35 (s, *C*$_{Mes}$), 137.7 (d, $^1J_{CP}$ = 25.1 Hz, *C*$_{ipso\ Ph}$), 137.6 (d, $^1J_{CP}$ = 114.7 Hz, *C*$_{ipso\ Ph}$), 136.75, 136.7, 136.6, 136.4, 136.3 (s, *C*$_{Mes}$), 133.4 (d, $J_{CP}$ = 9.0 Hz, *C*H$_{Ph}$), 132.6 (d, $J_{CP}$ = 9.0 Hz, *C*H$_{Ph}$), 132.5 (d, $J_{CP}$ = 3.0 Hz, *C*H$_{Ph}$), 132.2 (d, $J_{CP}$ = 3.0 Hz, *C*H$_{Ph}$), 130.9 (dd, $J_{CP}$ = 18.4 Hz, $J_{CRh}$ = 1.7 Hz, *C*H$_{Ph}$), 130.2 (br dd, $J_{CP}$ = 2.7 Hz, $J_{CRh}$ = 1.9 Hz, *C*H$_{Ph}$), 129.6 (s, *C*H$_{Ph}$), 129.5, 129.45, 129.40, 129.3 (s, *C*H$_{Mes}$), 129.3 (d, $J_{CP}$ = 10.1 Hz, *C*H$_{Ph}$), 128.7 (d, $J_{CP}$ = 11.1 Hz, *C*H$_{Ph}$), 127.6 (s, *C*$_{Im-4}$), 126.9 (dd, $^1J_{CP}$ = 62.4 Hz, $^2J_{CRh}$ = 3.0 Hz, *C*$_{Ph}$), 125.0 (d, $J_{CP}$ = 13.1 Hz, *C*H$_{Ph}$), 122.9 (s, CH$_{Im-5}$), 81.7 (s, Cp), 26.9 (s, PCH*C*H$_2$Im), 22.5 (dd, $^1J_{CP}$ = 32.2 Hz, $^1J_{CRh}$ = 24.1 Hz, P*C*HCH$_2$Im), 21.2, 18.9, 18.8, 18.6, 18.5 ppm (s, C*H*$_{3Mes}$). MS (ESI$^+$): *m/z*: 926.1 [M]$^+$; HRMS (ESI$^+$): calcd for $C_{50}H_{45}MnN_2O_4PRh$, 926.1552; found, 926.1564 ($\varepsilon_r$ = 1.3 ppm). IR (THF): $\nu_{CO}$ 2034, 1966, 1912, 1845 cm$^{-1}$. IR (toluene): $\nu_{CO}$ 2036, 1970, 1913, 1845 cm$^{-1}$.

## X-ray diffraction studies

The X-ray crystallographic data for all complexes were collected at −173°C using a Rigaku Synergy diffractometer (CuKα, 1.54184 Å) equipped with an Oxford Cryosystem. The structures have been solved by direct methods using SIR2018 program[2] and refined by means of least-square procedures on $F^2$ using SHELXL[3] integrated in WinGX 2018/3 system.[4] Absorption correction was performed using a Multiscan procedure.[5] All non-hydrogen atoms were refined anisotropically. Hydrogen atoms were initially refined with soft restraints on the bond lengths and angles to regularize their geometry and Uiso (H) (in the range 1.2-1.5 times Ueq of the parent atom), after which the positions were refined with riding model. After completion of the initial refinement for [**3b**](OTf) and **5a** it was found that *ca.* 7.0% of the overall cell volume was occupied by heavily disordered solvent molecules accounting for 102 and 42 electrons per unit cell, respectively. Since we were unable to find the reliable model in terms of discrete atomic sites, the contribution of the electron density in these space voids was minimized using the SQUEEZE procedure.[6] Detailed crystallographic data and structural refinement parameters are given in Table S1.

**Table S1.** Crystallographic details and refinement data for complexes [**3a**](OTf), [**3b**](OTf) and **5a**

| Complex | [**3a**](OTf) | [**3b**](OTf) | **5a** |
|---|---|---|---|
| Formula | $C_{49}H_{47}F_3MnN_2O_5PS$ | $C_{49}H_{65}F_3MnN_2O_5PS$ | $C_{54}H_{53}MnN_2O_5PRh$ |
| $M_w$ (g mol$^{-1}$) | 918.88 | 937.00 | 998.83 |
| T(K) | 100 | 100 | 100 |
| Crystal system | monoclinic | monoclinic | triclinic |
| Space group | P $2_1$/n | P $2_1$/c | P -1 |
| *a* (Å) | 30.6370(2) | 25.31460(10) | 12.51570(10) |
| *b* (Å) | 8.08020(10) | 8.53570(10) | 14.6557(2) |
| *c* (Å) | 35.4557(3) | 22.79300(10) | 15.2252(2) |
| *α* (°) | 90 | 90 | 107.4030(10) |
| *β* (°) | 93.0470(10) | 104.6720(10) | 110.8530(10) |
| *γ*(°) | 90 | 90 | 94.5710(10) |
| V (Å$^3$) | 8764.76(14) | 4764.46(7) | 2435.42(5) |
| Z | 8 | 4 | 2 |
| $\rho_{calcd}$ (g cm$^{-3}$) | 1.393 | 1.306 | 1.362 |
| μ (mm$^{-1}$) | 3.765 | 3.464 | 5.546 |
| Collected reflns | 142973 | 145757 | 77758 |
| Unique reflns | 17843 | 9576 | 9608 |
| $R_{int}$ | 0.075 | 0.044 | 0.043 |
| Nb of parameters | 1129 | 638 | 583 |
| Nb of reflns ($I$≥2σ) | 14317 | 9074 | 9172 |
| Final *R*, *wR* ($I$≥2σ) | 0.0538/0.1431 | 0.0555/0.1656 | 0.0310/0.0843 |
| *R*, *wR* (all data) | 0.0684/0.1524 | 0.0585/0.1689 | 0.0329/0.0852 |
| $\Delta\rho_{min}$/ $\Delta\rho_{max}$ | −0.86/1.01 | −0.67/0.82 | −0.83/0.93 |
| GOF | 1.014 | 0.882 | 1.030 |
| CCDC Number | 2393836 | 2393837 | 2393838 |

## Electrochemical investigations

Voltammetric measurements were carried out with a potentiostat Autolab PGSTAT100 controlled by GPES 4.09 software. Experiments were performed at room temperature in a homemade airtight three-electrode cell consisting of a Pt working electrode (d = 0.5 mm), a platinum wire (S = 1 $cm^2$) as counter electrode, and a saturated calomel electrode (*SCE*) separated from the solution by a bridge compartment as a reference. Before each measurement, the working electrode was cleaned with a polishing machine (Presi P230, P4000). The measurements were carried out in dry $CH_3CN$ under argon atmosphere using 0.1 M [$n$$Bu_4N$]($PF_6$) (Fluka, 99% puriss electrochemical grade) as supporting electrolyte and typically $10^{-3}$ M sample concentration.

## DFT calculations.

Calculations were performed with the Gaussian 09[7] package at the DFT/ωB97XD[8] level using Def2-TZVP basis set[9] for all atoms supplemented with the effective core potential (ECP)[10] for rhodium atom without any ligand simplification. The structures of all complexes were fully optimized in toluene (ε = 2.37) described by the SMD model[11] without any symmetry restrictions. The nature of minima points on the potential energy surfaces was confirmed by vibrational analysis. ETS-NOCV analysis[12] of interaction energy was performed with ORCA 5.04 software package[13] on the same level (ωB97-D3/Def2-TZVP(ECP(Rh))/SMD(toluene)) on the G09 geometry of complex. The deformation density plots were further calculated (by scaling of interacting orbitals by their eigenvalue factor, with subsequent subtraction of their squared values) and plotted with the Chemcraft 1.8 program.[14] QTAIM analysis was performed by AIMALL[15] and Multiwfn 3.8[16] packages. NBO charges was obtained by NBOPro v.6 software.[17]

The optimized geometries of complexes are shown in Figure S1 and the pertinent values of bond distances and AIM/NBO6 charges are collected in Table S2. Calculated metal-carbene and metal-ylide bond distances in complex **5a** correspond well to those obtained from X-ray diffraction experiment with a maximal deviation of 0.025 Å. DFT data showed that cyclometallated Rh(I) complex can exist as two rotamers **6a** and **6a'** different by the position of the [$Rh(CO)_2$] moiety relative to the NHC plane (Figure S1). According to $\Delta G^{298}$, complex **6a** is 3.7 and 4.8 kcal/mol more thermodynamically stable than its isomer **6a'** and the starting ditopic NHC derivative **5a**, respectively.

**Table S2.** Selected bond lengths and charges for optimized complexes **4a**, **4b**, **5a**, **5b** and **6a/6a'**

| Complex | Selected bond distances (Å) | | | | AIM and NBO6 (in parenthesis) charges | | | | |
|---|---|---|---|---|---|---|---|---|---|
| | Mn−NHC | M−*a*NHC | M−ylide | P−$C_{ylide}$ | Mn | NHC | [$Rh(CO)_2$] | $CO_{trans}$[a] | $CO_{cis}$[a] |
| **4a** | 2.035 | 1.994 | 2.159 | 1.692 | 0.971 (−0.493) | −1.657 (−0.930) | – | – | – |
| **4b** | 2.035 | 1.990 | 2.127 | 1.708 | 0.970 (−0.494) | −1.660 (−0.928) | – | – | – |
| **5a** | 2.007 | 2.063 | 2.215 | 1.784 | 0.970 (−0.496) | −1.361 (−0.581) | 0.177 (0.173) | −0.160 (0.135) | −0.207 (0.075) |
| **5b** | 2.028 | 2.061 | 2.232 | 1.780 | 0.970 (−0.496) | −1.363 (−0.583) | 0.171 (0.162) | −0.159 (0.135) | −0.225 (0.051) |
| **6a** | 2.006 | – | 2.203 | 1.781 | 0.968 (−0.499) | −1.065 (−0.381) | 0.176 (0.168) | −0.171 (0.129) | −0.188 (0.096) |
| **6a'** | 1.997 | – | 2.185 | 1.787 | 0.965 (−0.502) | −1.101 (−0.402) | 0.176 (0.184) | −0.178 (0.119) | −0.182 (0.107) |

[a] The *cis*- and *trans*-arrangement of CO ligands is given related to the phosphonium ylide moiety

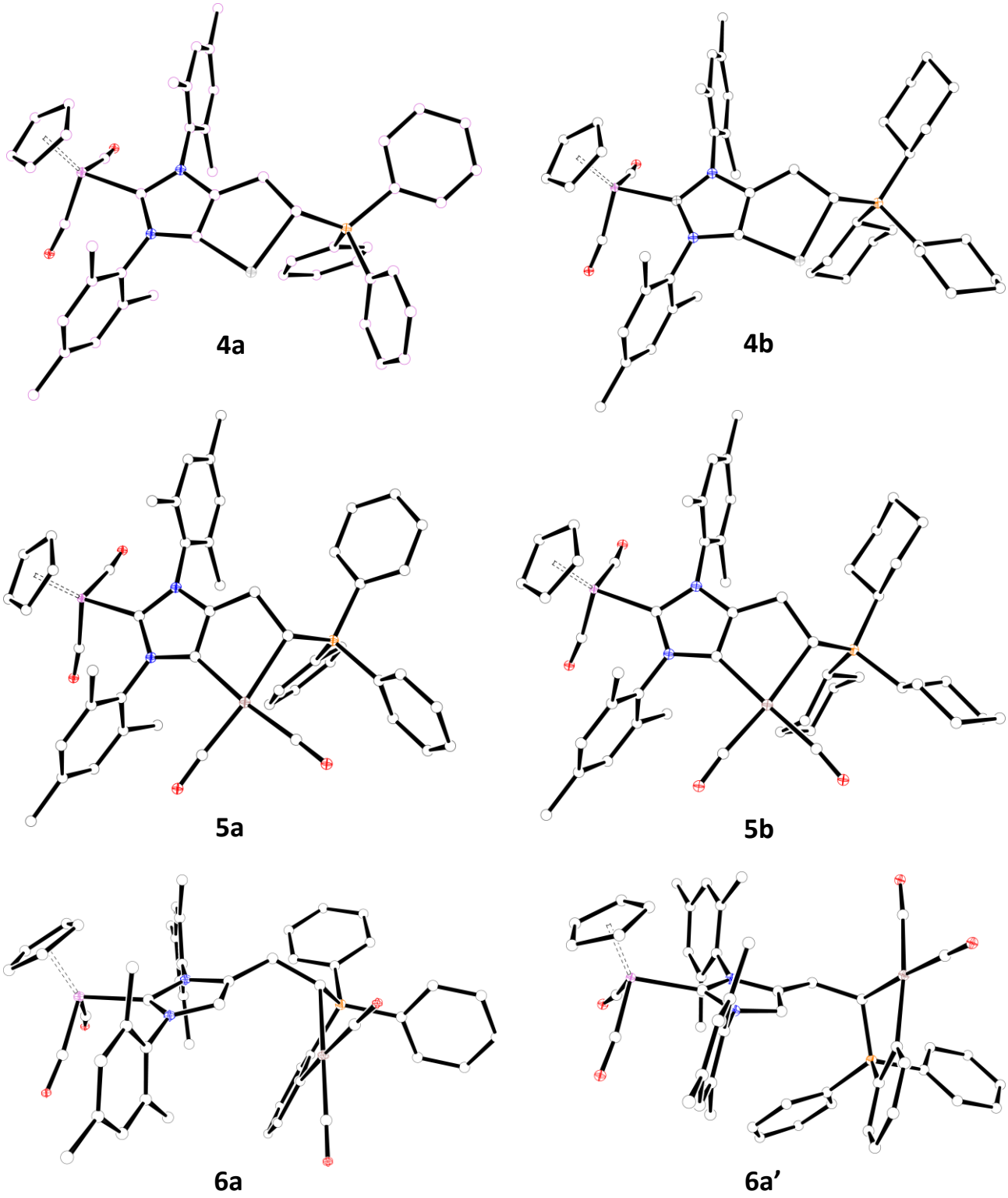


**Figure S1**. Optimized structures of complexes **4a**, **4b**, **5a**, **5b** bearing anionic *d*NHC ligands and two conformers of cyclometallated derivatives **6a**/**6a'** (hydrogen atoms are not shown). Element color codes: Li – grey, C – white, N – blue, O – red, P – orange, Mn – violet, Rh – brown.

Analysis of structural data for calculated NHC-ylide complexes revealed *ca.* 0.06-0.10 Å shorter metal-NHC and metal-ylide bonds for the adducts **4a-b** than for their Rh(I) congeners **5a-b**, which may be related to a stronger contribution of electrostatic interactions. As expected, lower acceptor ability of $Li^+$ cation *vs.* $[Rh(CO)_2]$ moiety can be also reflected from the accumulation of negative charge in the ditopic NHC fragment of **4a-b** (Table S2) and significant double bond character of P–C ylide bonds being *ca.* 0.07-0.08 Å shorter than for their related Rh(I) derivatives **5a-b**.

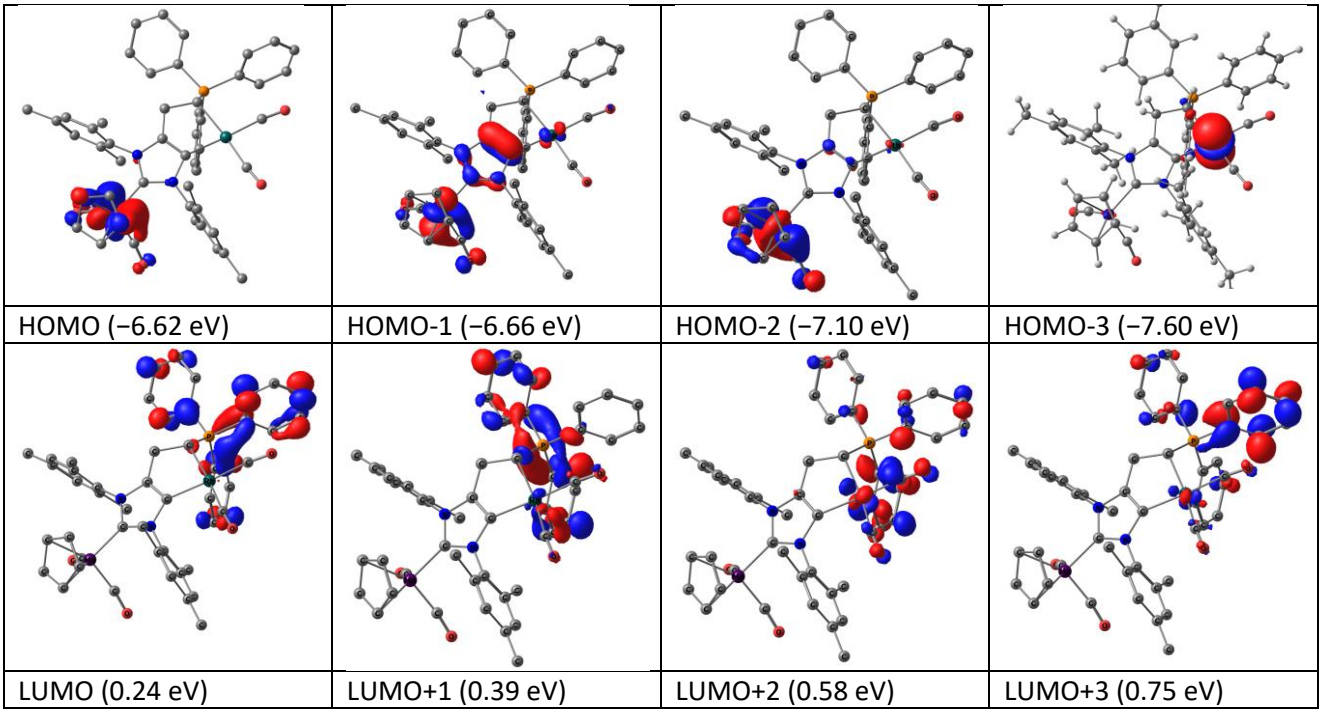


**Figure S2**. Selection of molecular orbitals for bimetallic complex **5a** with isosurface set at 0.05 a.u. and their energies in eV (in parenthesis).

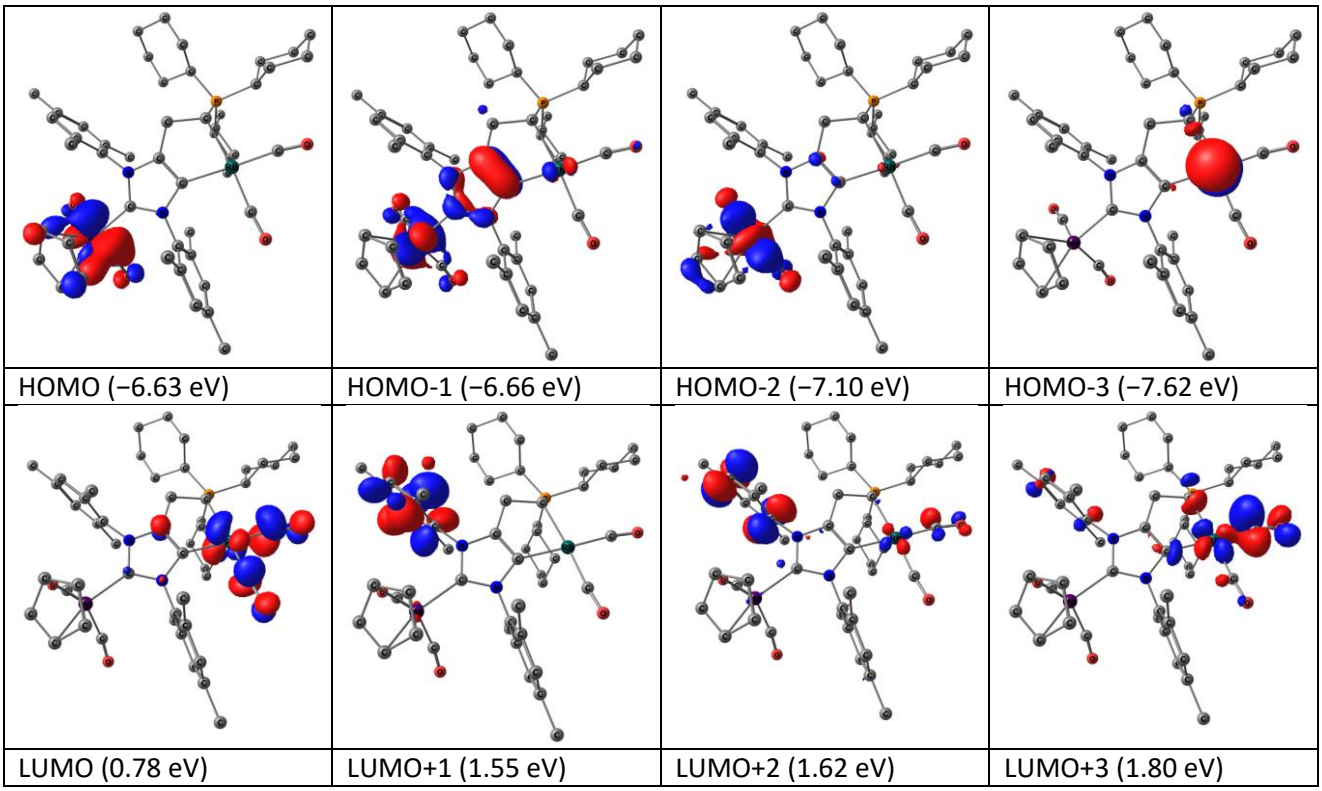


**Figure S3**. Selection of molecular orbitals for bimetallic complex **5b** with isosurface set at 0.05 a.u. and their energies in eV (in parenthesis).

Selected near frontier molecular orbitals for complexes **5a** and **5b** as well as their related energies are presented in Figure S2 and S3, respectively. While HOMO and HOMO-2 are centered uniquely at the [Cp(CO)$_2$Mn] moiety, a significant contribution of *d*NHC ligand may be noticed for HOMO-1, whereas HOMO-3 represents essentially $d_{z^2}$ orbital of the rhodium atom. Interestingly,

all low-lying LUMOs for complex **5a** are located at the cationic $^{+}PPh_3$ fragment (Figure S2, *down*) being in agreement with the observed reactivity of this site on a highly electron-rich Rh(I) center. In contrast, all accessible LUMO orbitals for complex **5b** are located either on the $[Rh(CO)_2]$ moiety or at the aromatic NHC substituents (Figure S3, *down*) thus explaining higher chemical robustness of complexes incorporating $PCy_3$-based ylide ligands.

Main primary NOCV channels for the bonding of $[Rh(CO)_2]$ fragment with bidentate *a*NHC-ylide ligands in **5a-b** are presented in Figures S4 and S5. The overall *ca.* 5:1 ratios between the associated energies responsible for σ-donation (Figure S4) and π-retrodonation (Figure S5) in complexes **5a-b** are close to those previously calculated using the same approach for the bonding of $[Cp(CO)_2Fe]^{+}$ fragment with neutral (4.8:1) and anionic (5.6-6.2:1) *a*NHC ligands.[18]

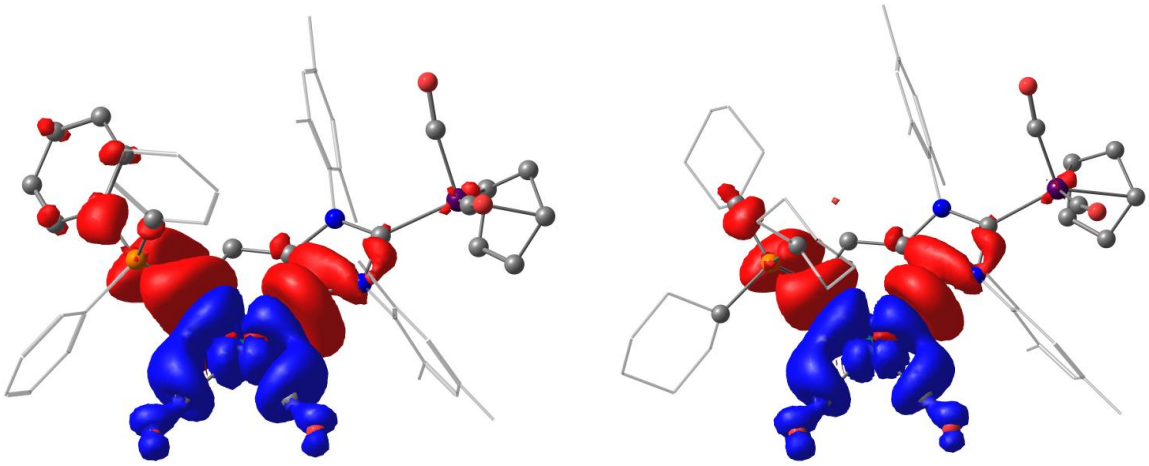

**NOCV1** **5a** (E = −72.018) **5b** (E = −70.947)

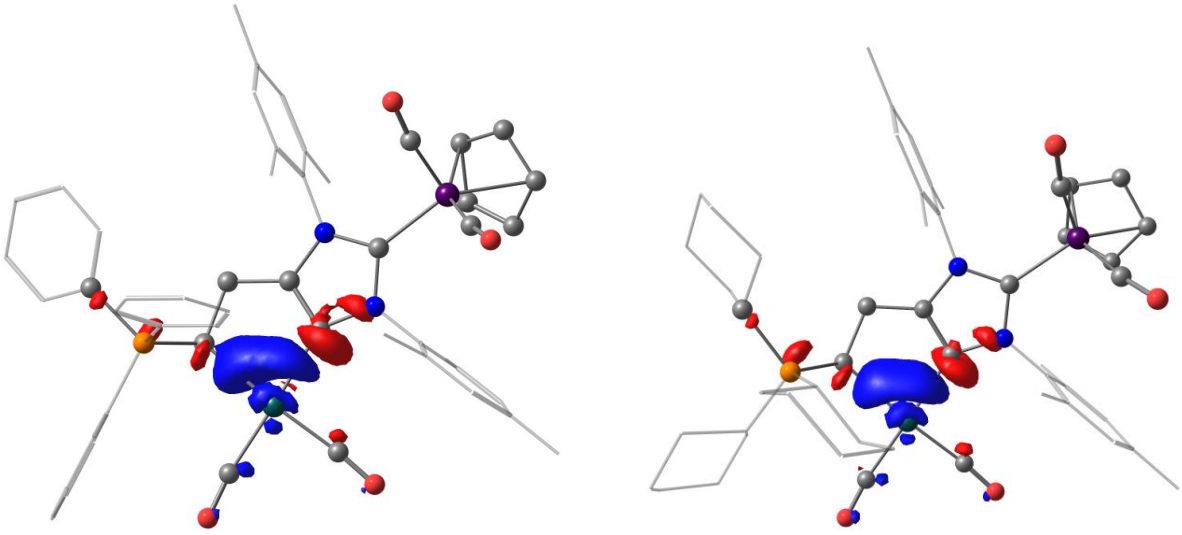

**NOCV2** **5a** (E = −43.269) **5b** (E = −43.472)

**Figure S4**. Electron deformation density (as isosurface at 0.001 a.u., red - electron density depletion, blue - electron density accumulation) corresponding to primary NOCV channels in bimetallic complexes **5a** (left) and **5b** (right) responsible for σ-donation to the $[Rh(CO)_2]$ fragment (associated energies in kcal/mol are given in parenthesis).

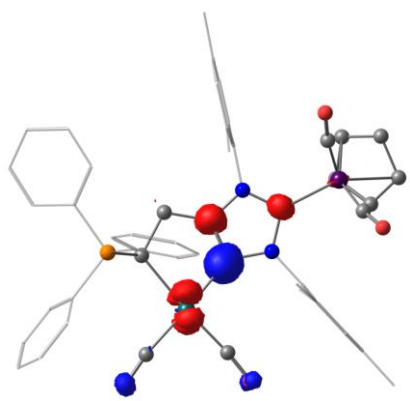

**NOCV3** **5a** (E = −6.013)

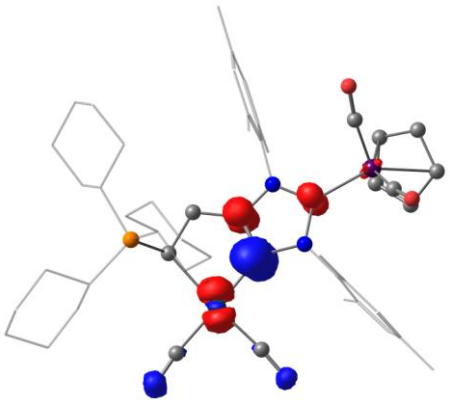

**5b** (E = −6.894)

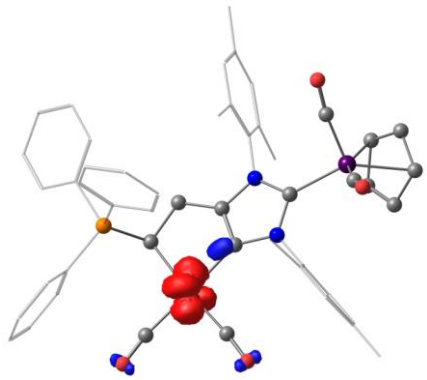

**NOCV4** **5a** (E = −6.692)

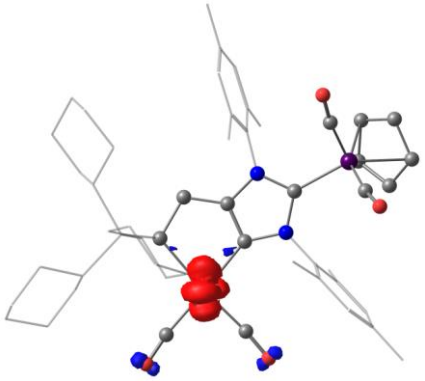

**5b** (E = −6.958)

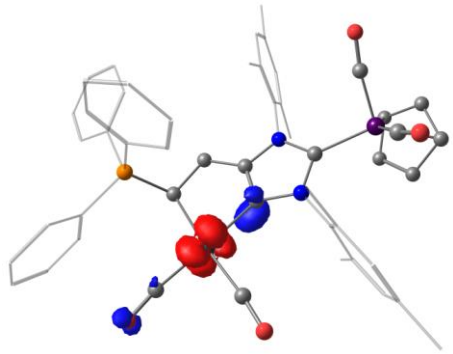

**NOCV5** **5a** (E = −5.925)

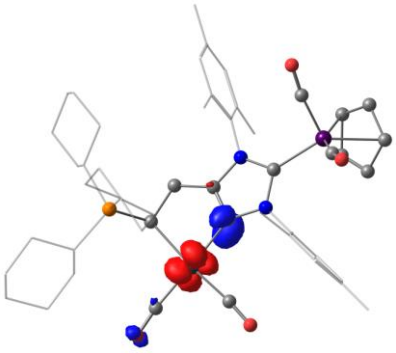

**5b** (E = −6.190)

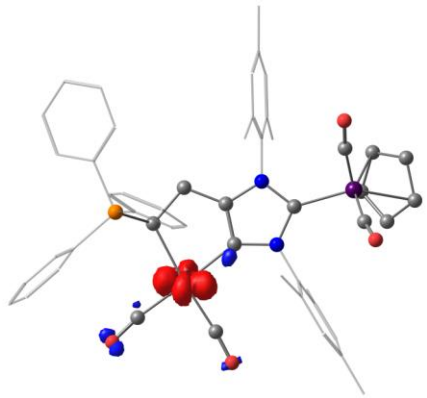

**NOCV5** **6a** (E = −4.776)

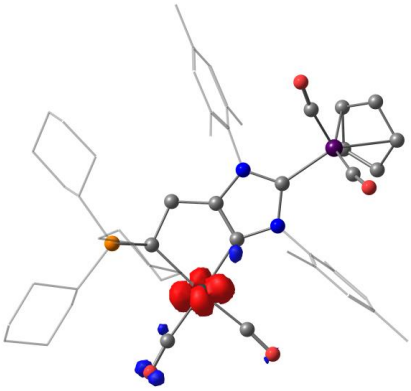

**5b** (E = −5.072)

**Figure S5**. Electron deformation density (as isosurface at 0.001 a.u., red - electron density depletion, blue - electron density accumulation) corresponding to primary NOCV channels in bimetallic complexes **5a** (left) and **5b** (right) responsible for π-back donation to the [$Rh(CO)_2$] fragment (associated energies in kcal/mol are given in parenthesis).

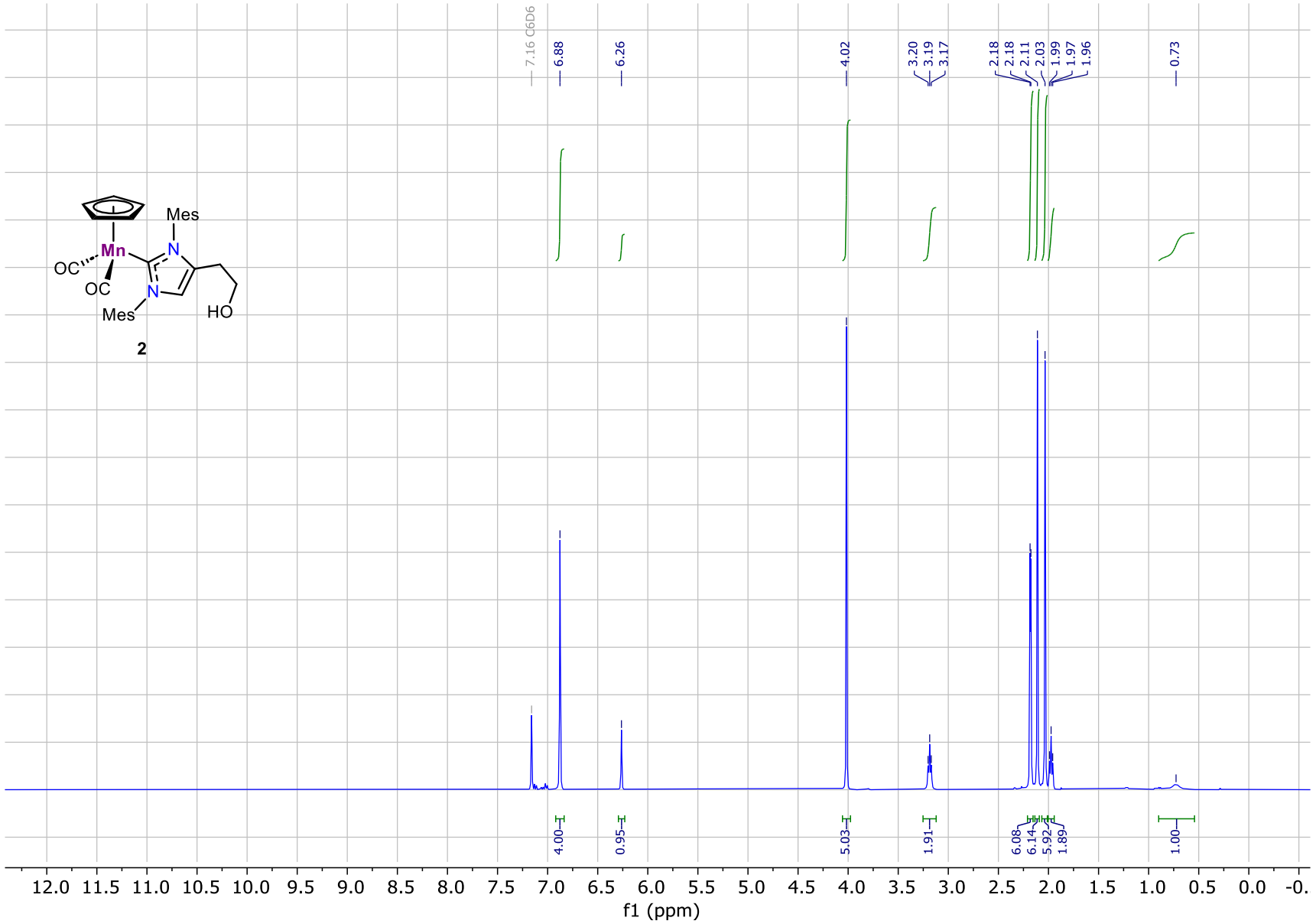


**Figure S6**. $^{1}H$ NMR spectrum of complex **2** (400.1 MHz, $C_6D_6$, 25°C).

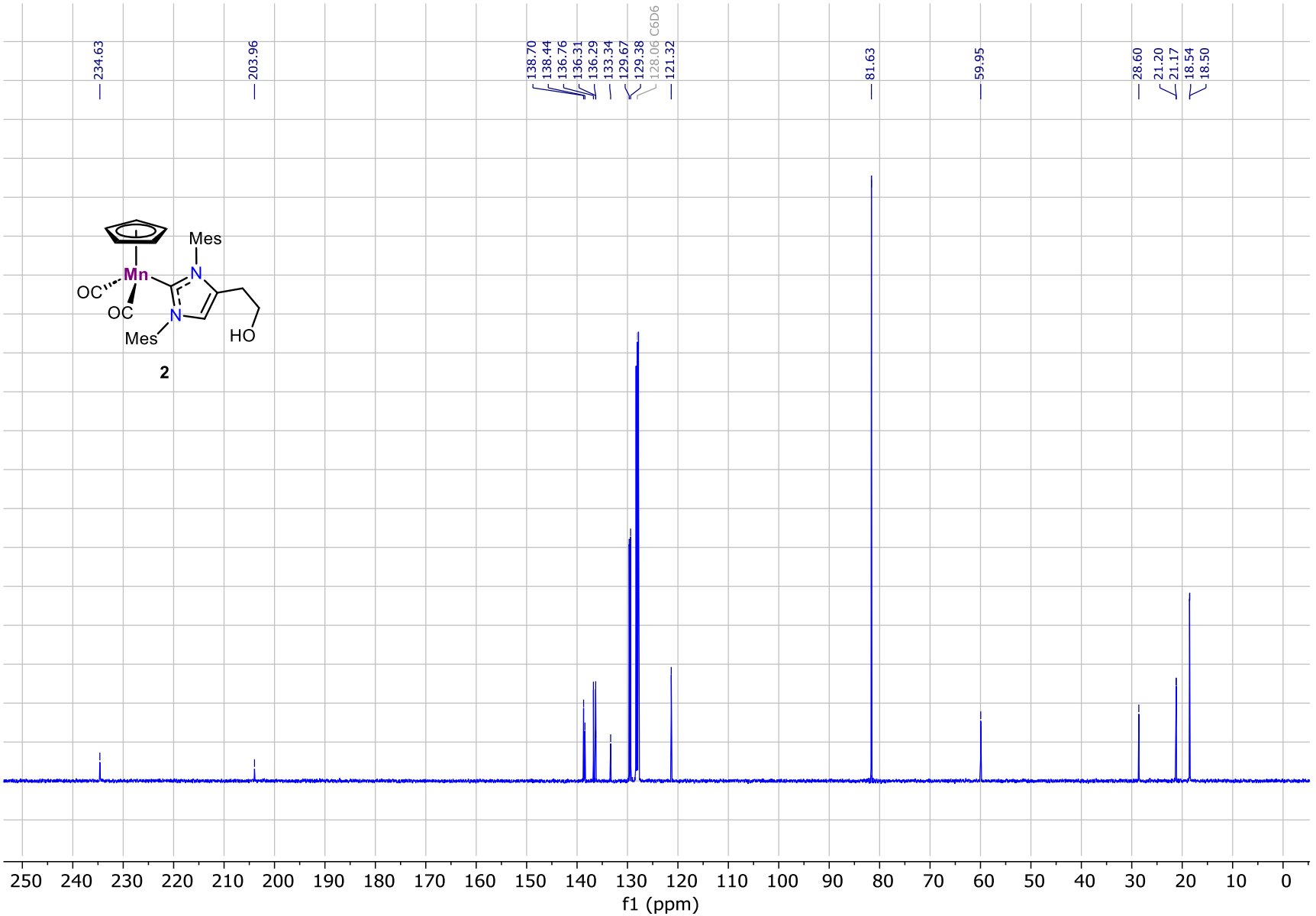


**Figure S7**. $^{13}C\{^{1}H\}$ NMR spectrum of complex **2** (100.6 MHz, $C_6D_6$, 25°C).

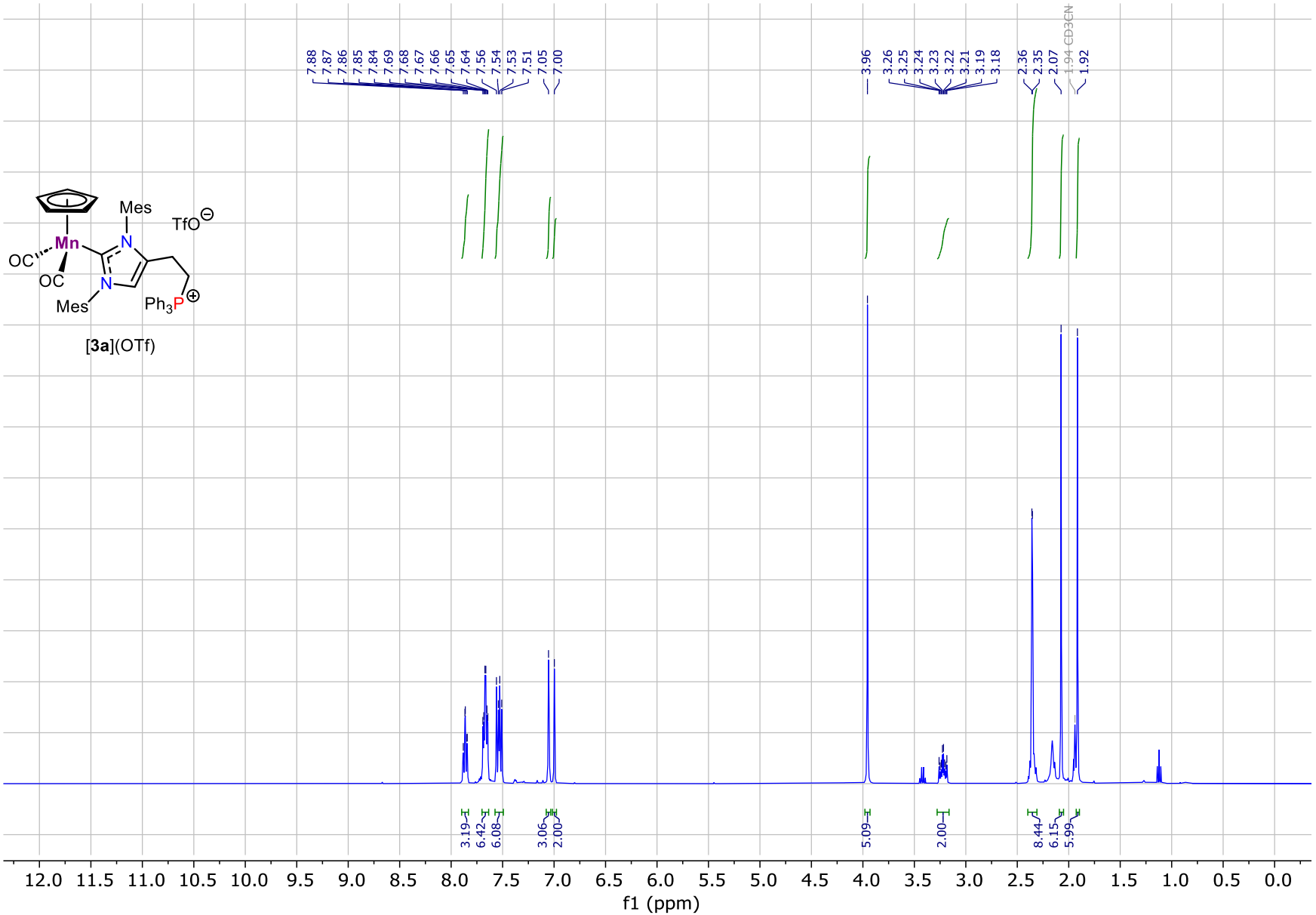


**Figure S8**. $^{1}H$ NMR spectrum of complex [**3a**](OTf) (400.1 MHz, $CD_3CN$, 25°C).

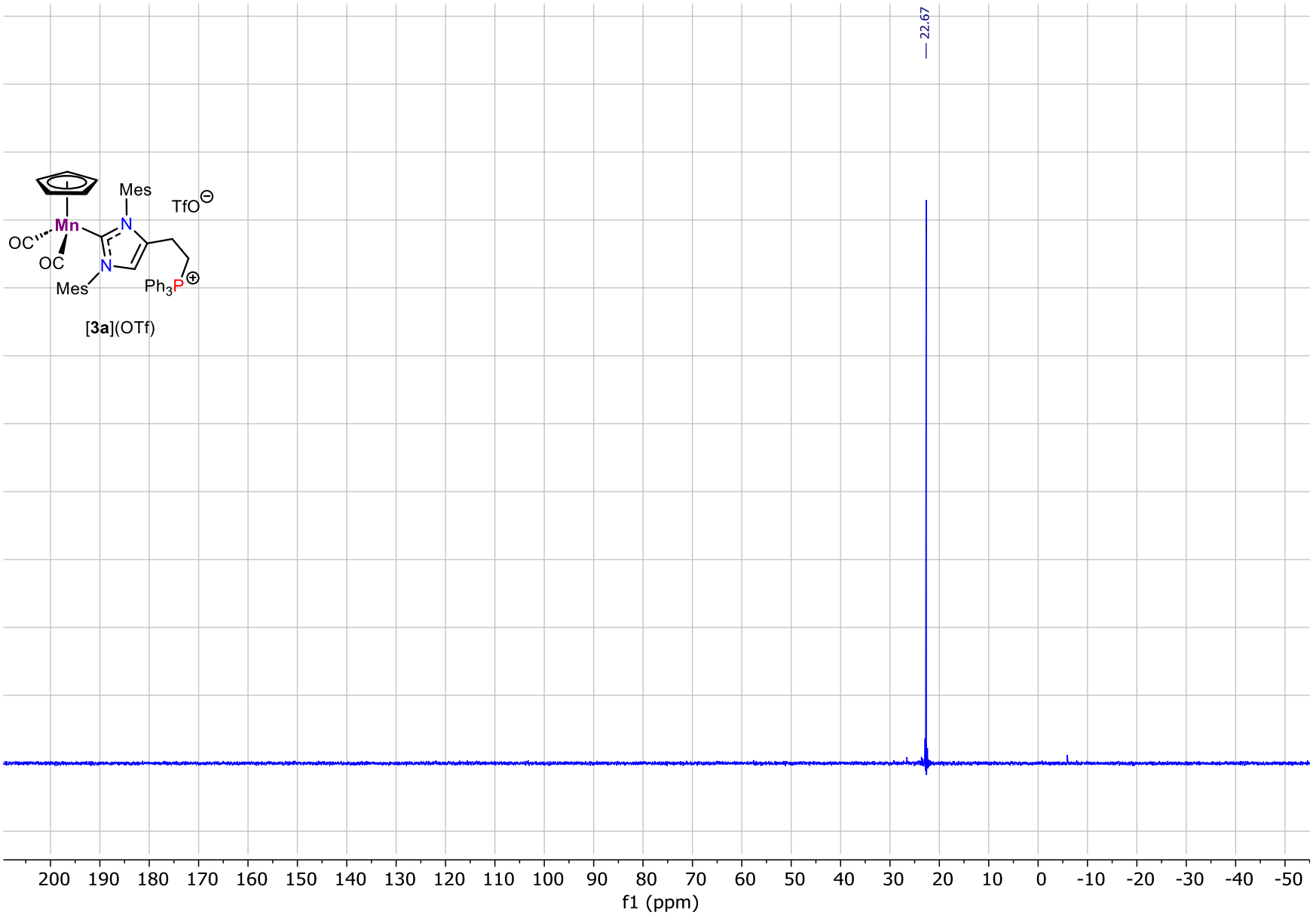


**Figure S9**. $^{31}P\{^{1}H\}$ NMR spectrum of complex [**3a**](OTf) (162.0 MHz, $CD_3CN$, 25°C).

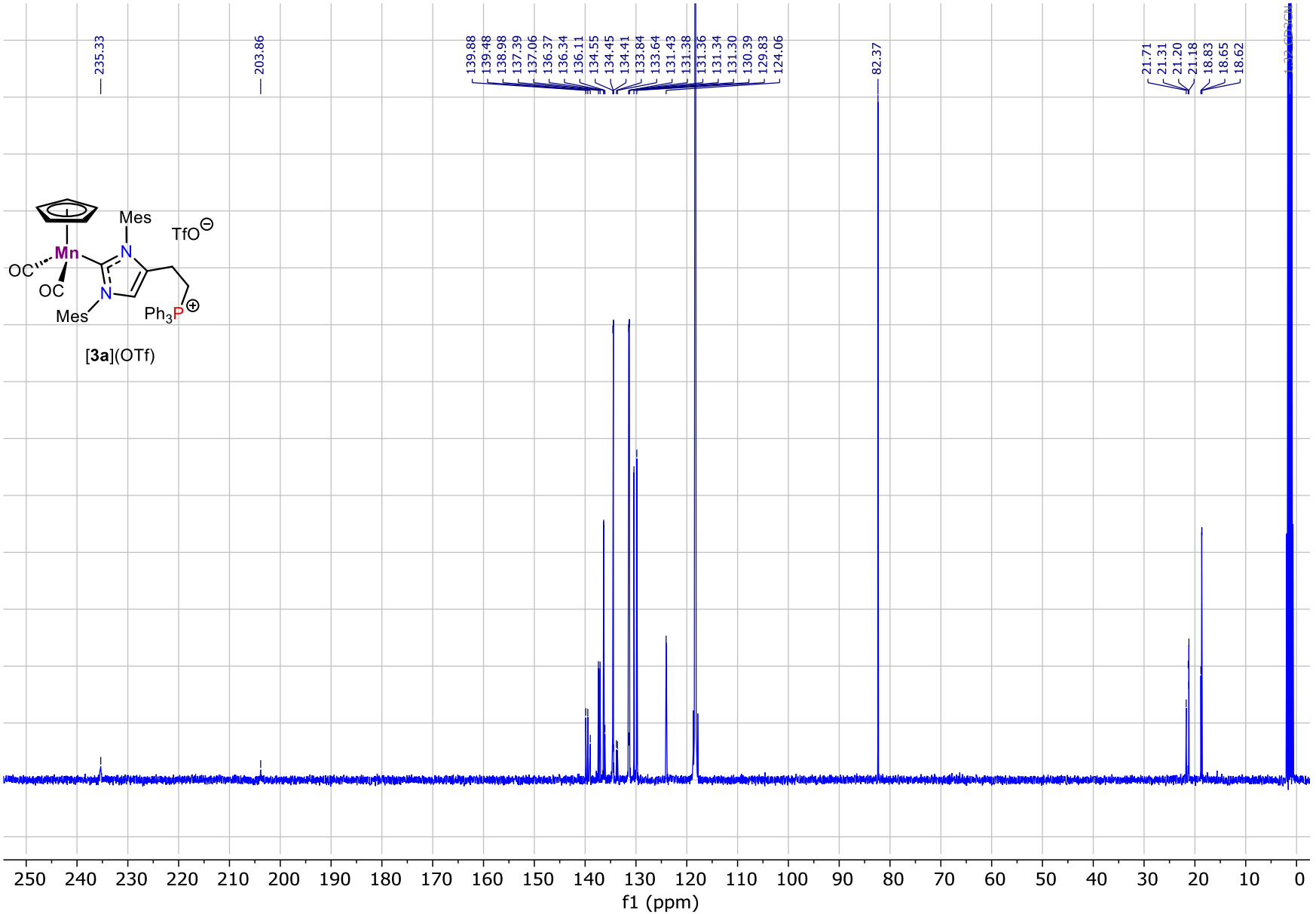


**Figure S10**. $^{13}C\{^{1}H\}$ NMR spectrum of complex [**3a**](OTf) (100.6 MHz, $CD_3CN$, 25°C).

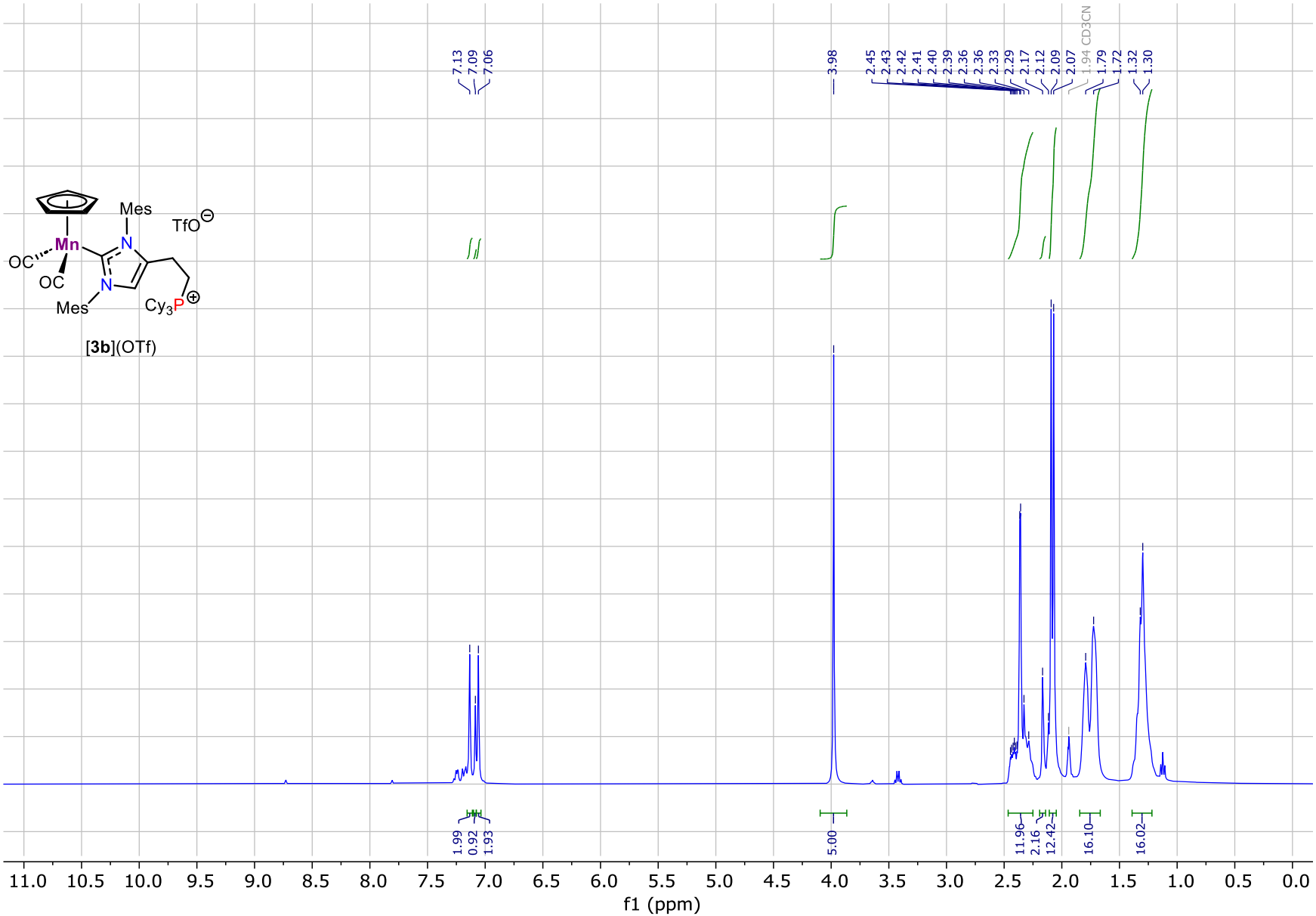


**Figure S11**. $^{1}$H NMR spectrum of complex [**3b**](OTf) (400.1 MHz, $CD_3CN$, 25°C).

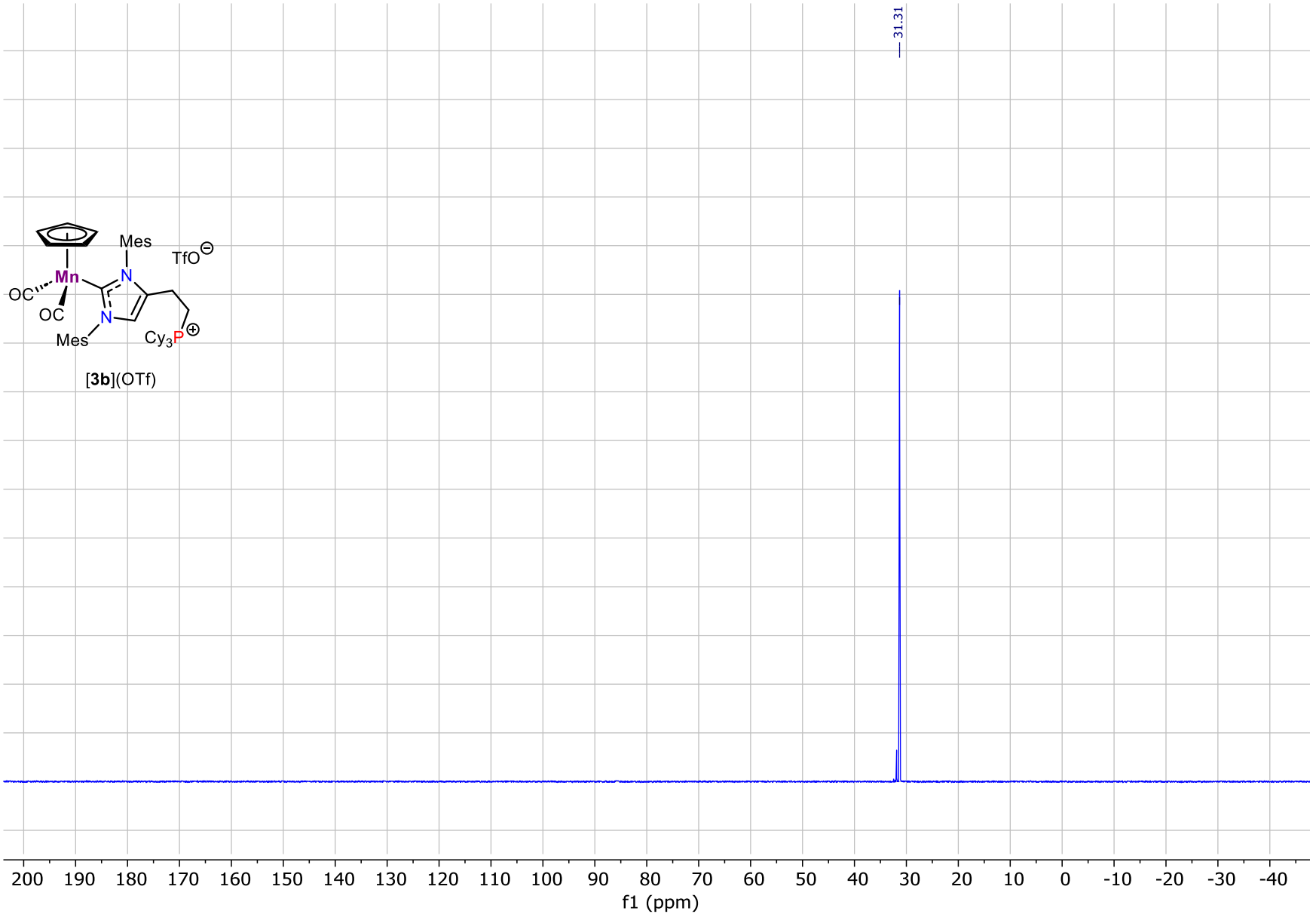


**Figure S12**. $^{31}P\{^{1}H\}$ NMR spectrum of complex [**3b**](OTf) (162.0 MHz, $CD_3CN$, 25°C).

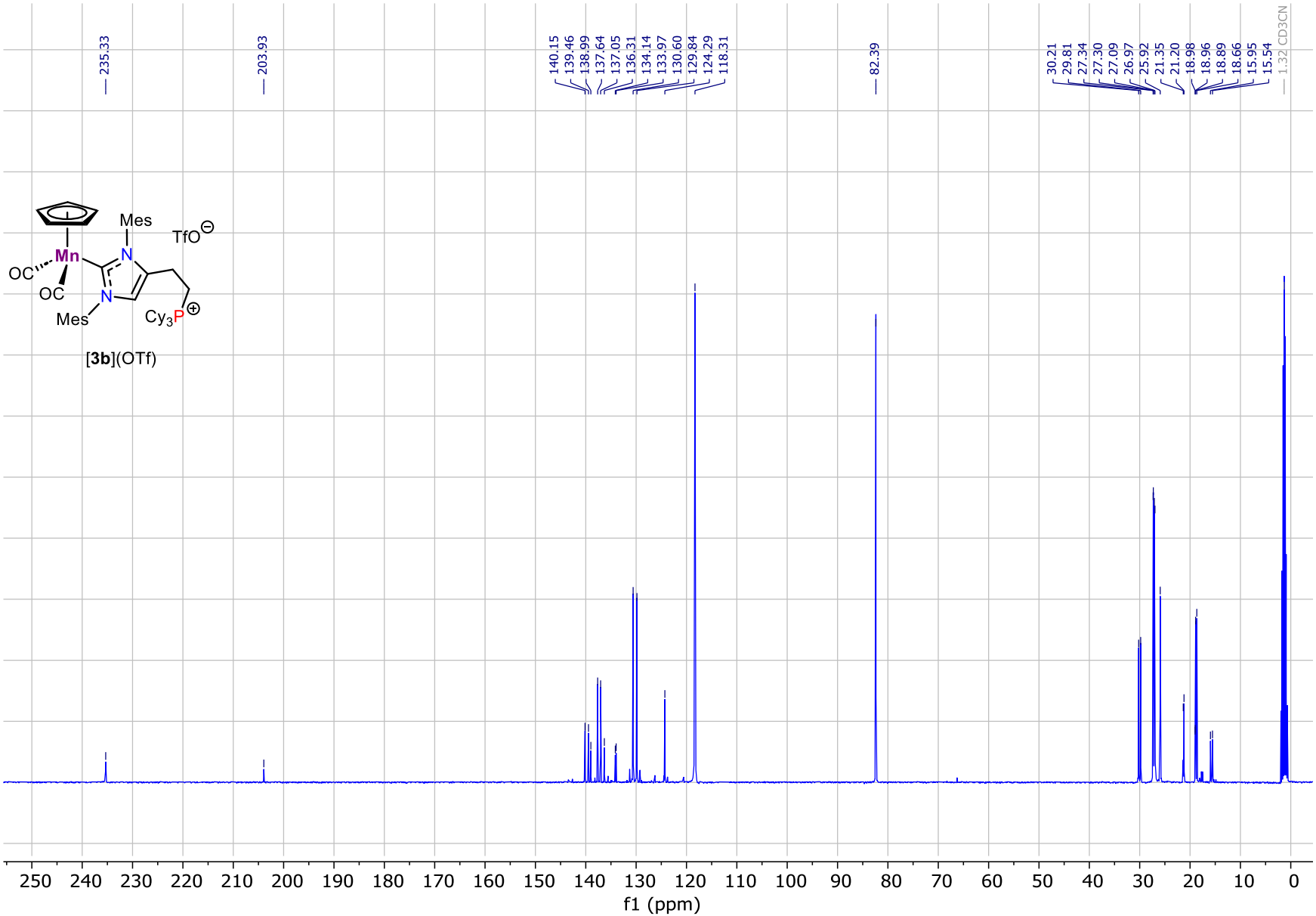


**Figure S13**. $^{13}C\{^{1}H\}$ NMR spectrum of complex [**3a**](OTf) (100.6 MHz, $CD_3CN$, 25°C).

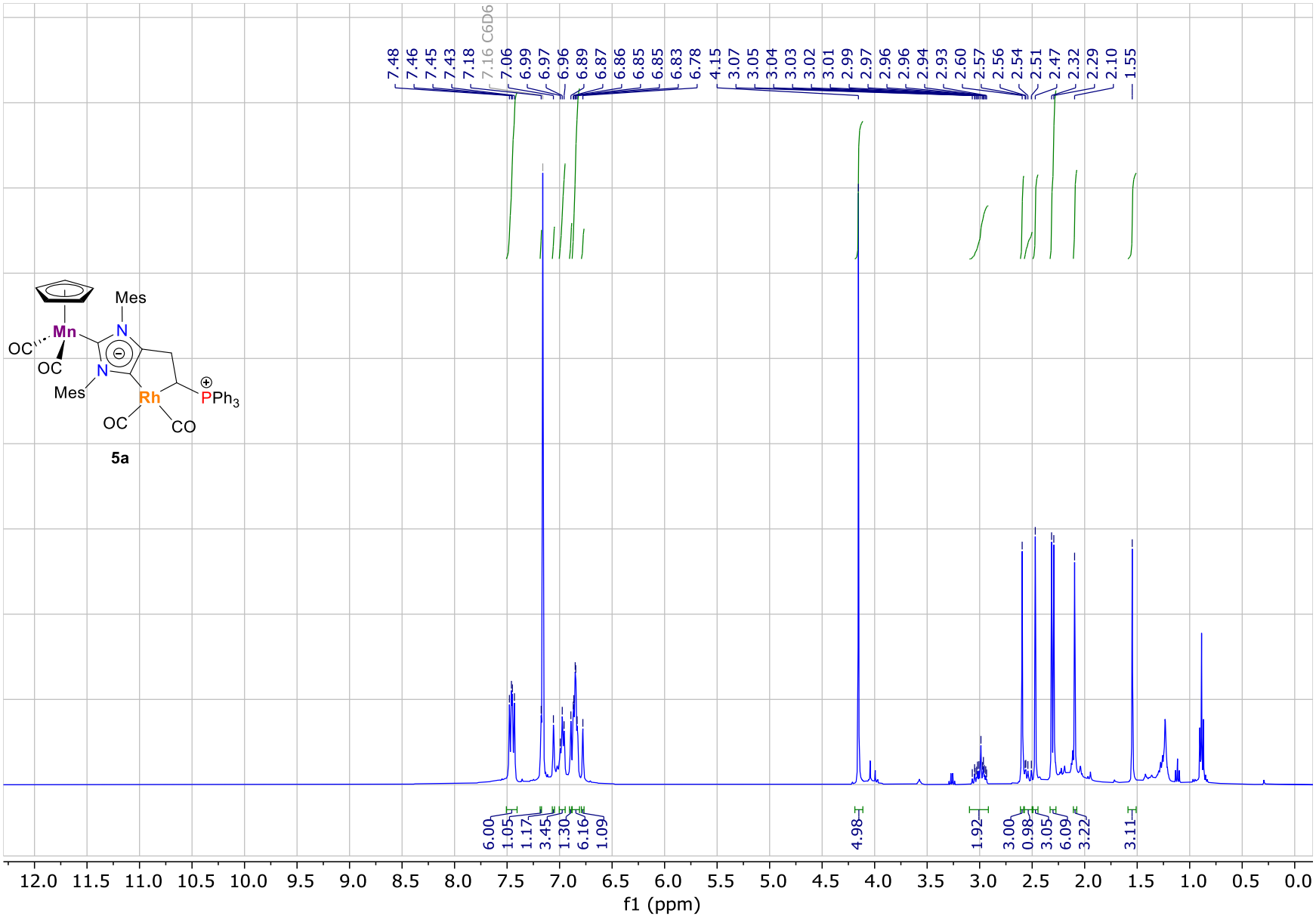


**Figure S14**. $^{1}H$ NMR spectrum of complex **5a** (400.1 MHz, $C_6D_6$, 25°C).

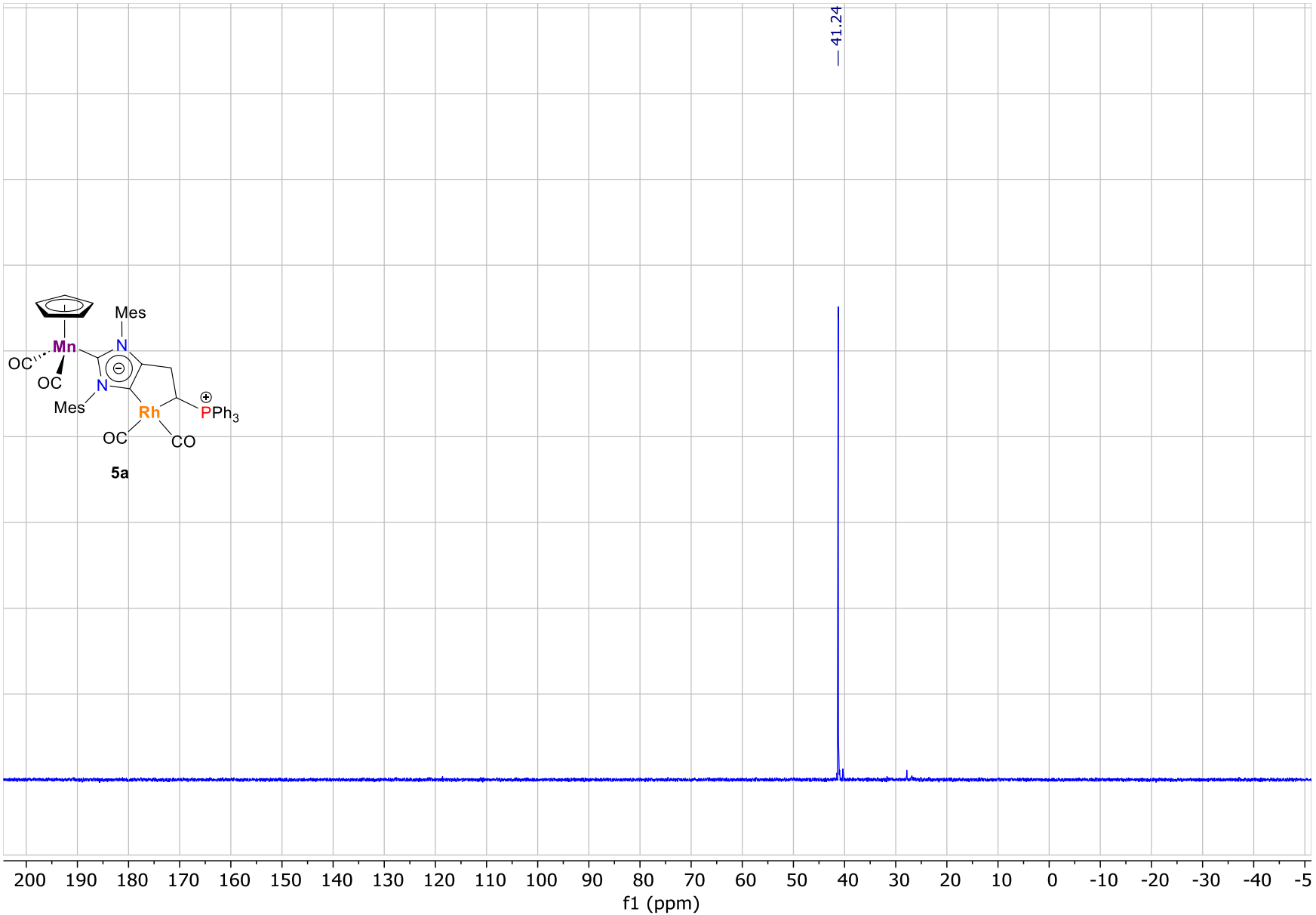


**Figure S15**. $^{31}P\{^{1}H\}$ NMR spectrum of complex **5a** (162.0 MHz, $C_6D_6$, 25°C).

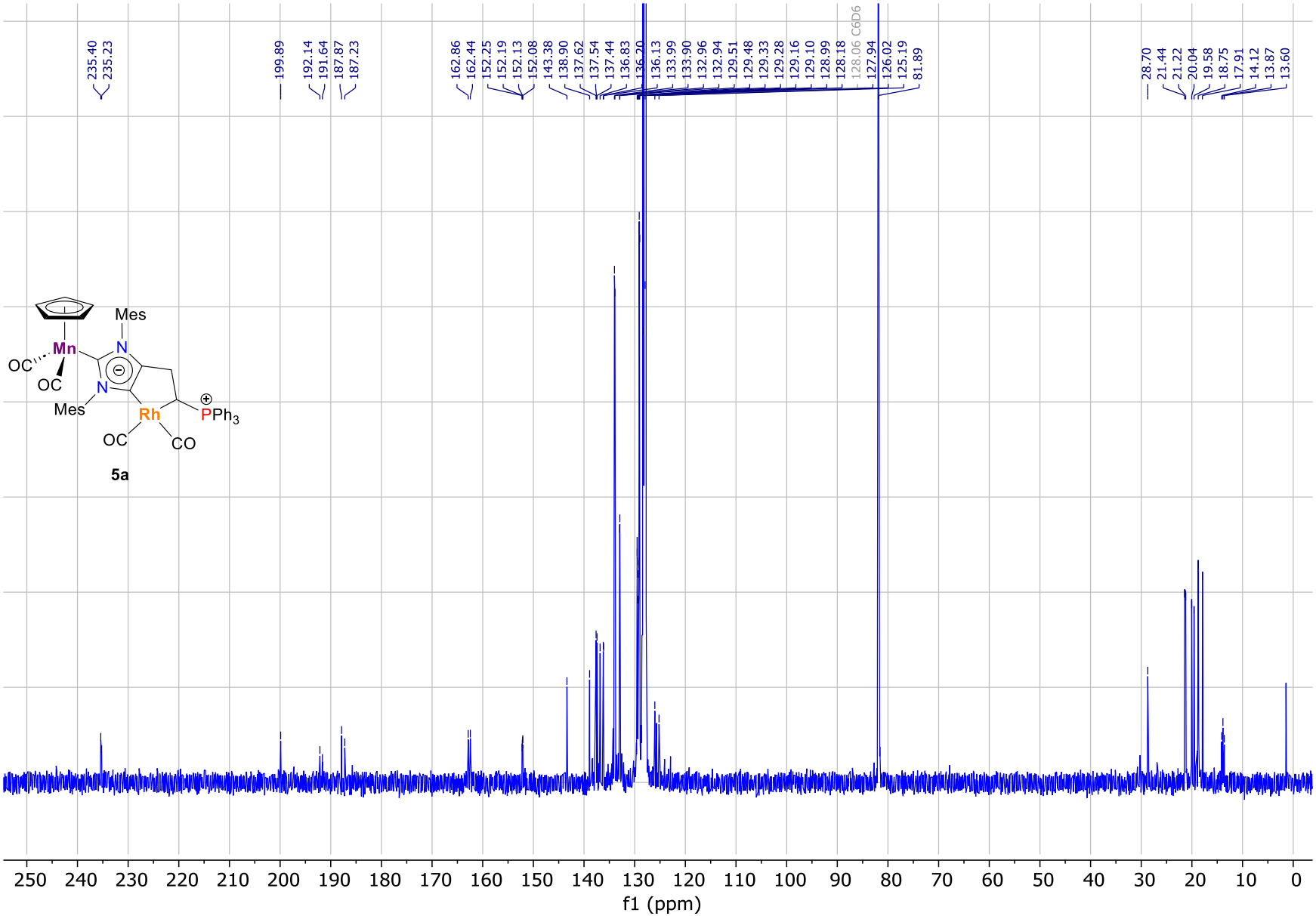


**Figure S16**. $^{13}C\{^{1}H\}$ NMR spectrum of complex **5a** (100.6 MHz, $C_6D_6$, 25°C).

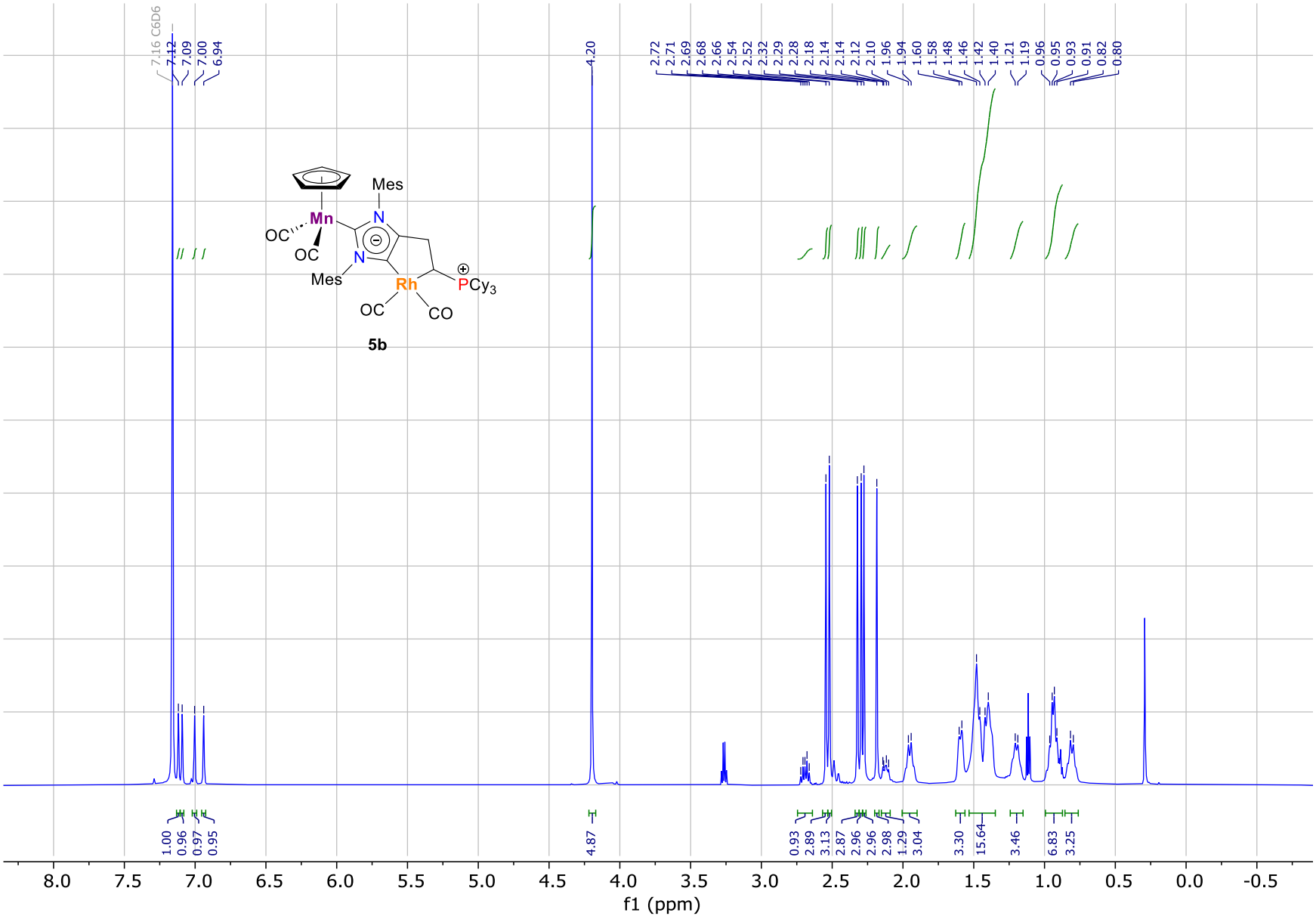


**Figure S17**. $^{1}H$ NMR spectrum of complex **5b** (600.2 MHz, $C_6D_6$, 25°C).

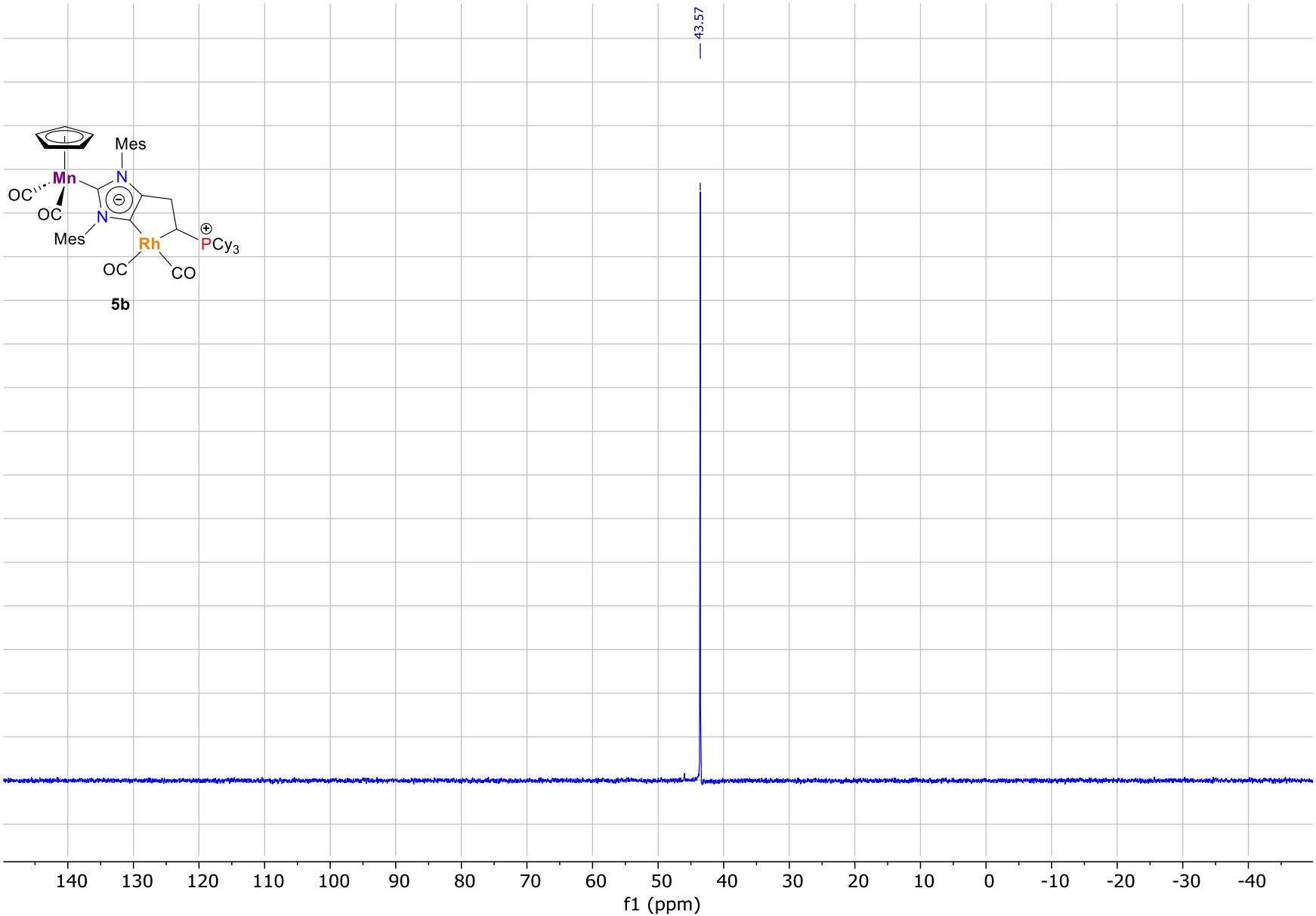


**Figure S18**. $^{31}P\{^{1}H\}$ NMR spectrum of complex **5b** (243.0 MHz, $C_6D_6$, 25°C).

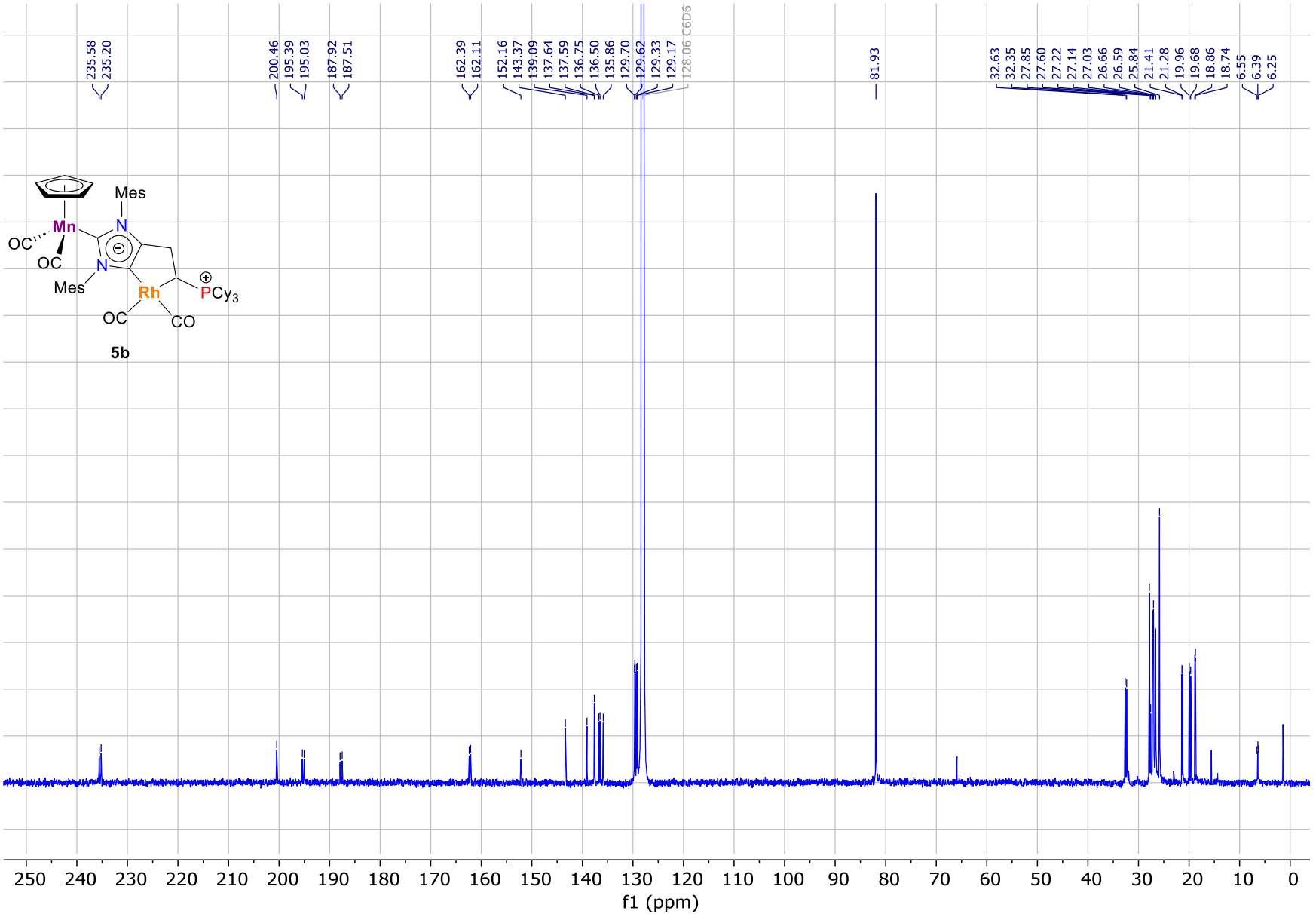


**Figure S19**. $^{13}C\{^{1}H\}$ NMR spectrum of complex **5b** (150.9 MHz, $C_6D_6$, 25°C).

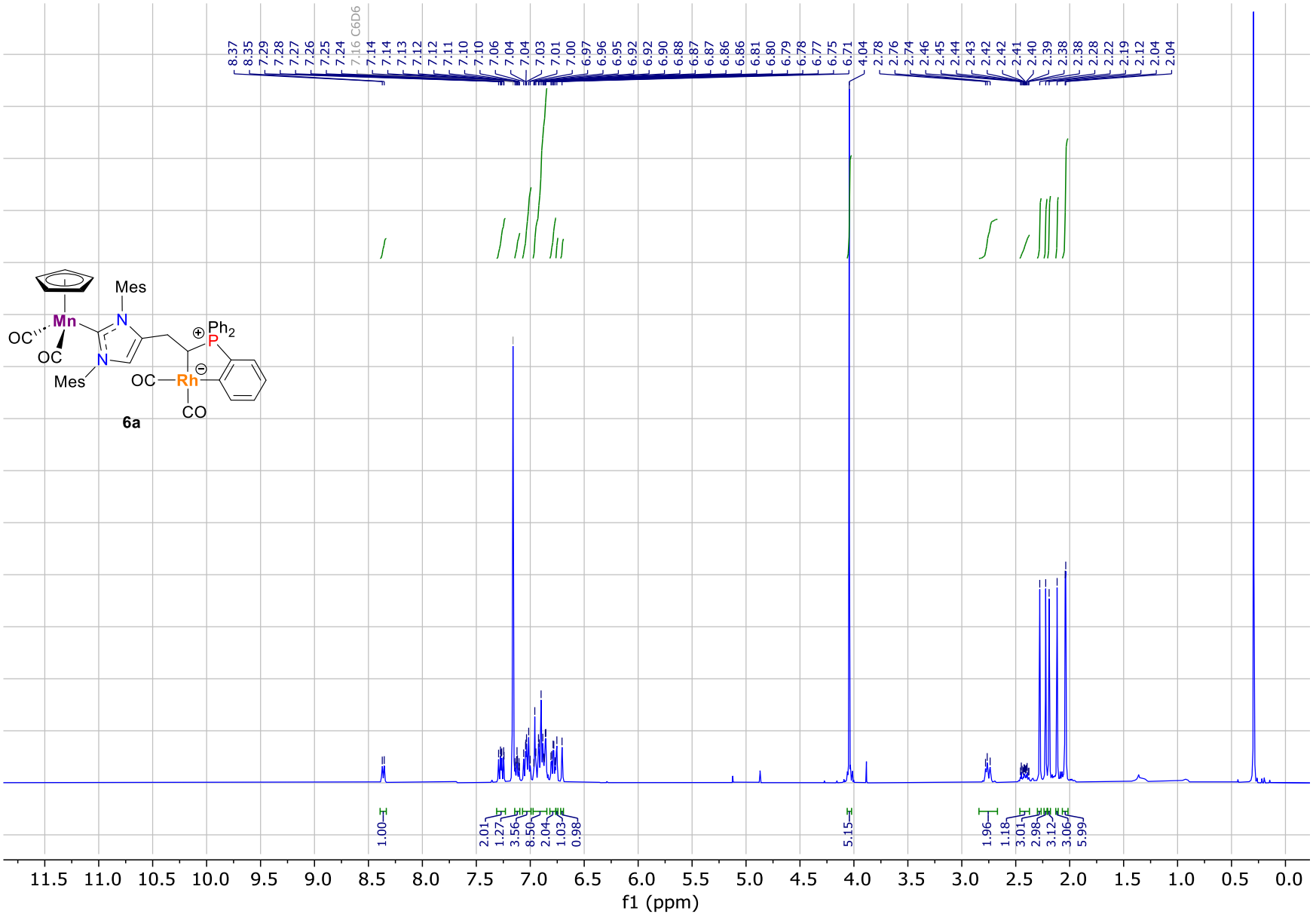


**Figure S20**. $^{1}H$ NMR spectrum of complex **6a** (400.1 MHz, $C_6D_6$, 25°C).

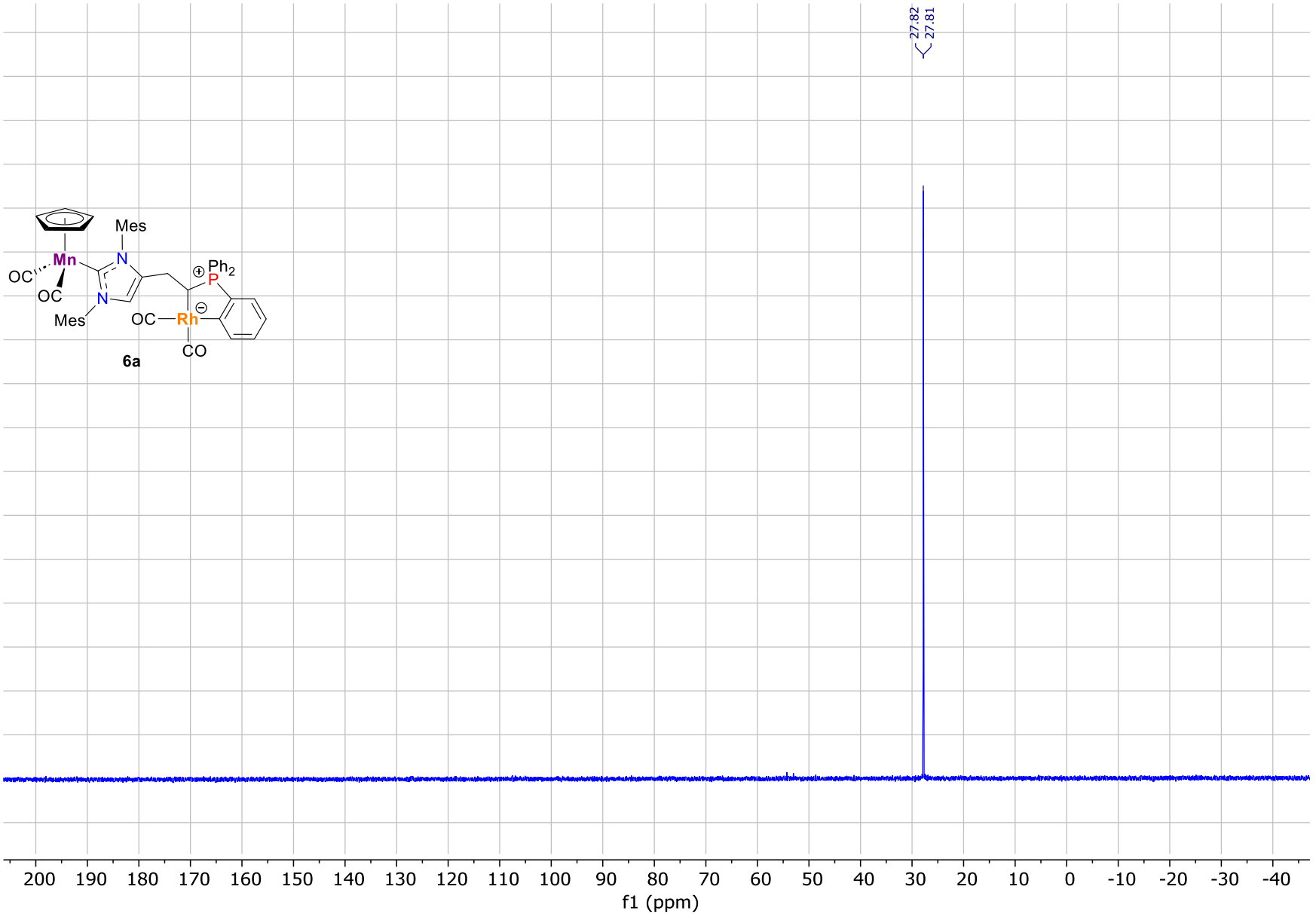


**Figure S21**. $^{31}P\{^{1}H\}$ NMR spectrum of complex **6a** (162.0 MHz, $C_6D_6$, 25°C).

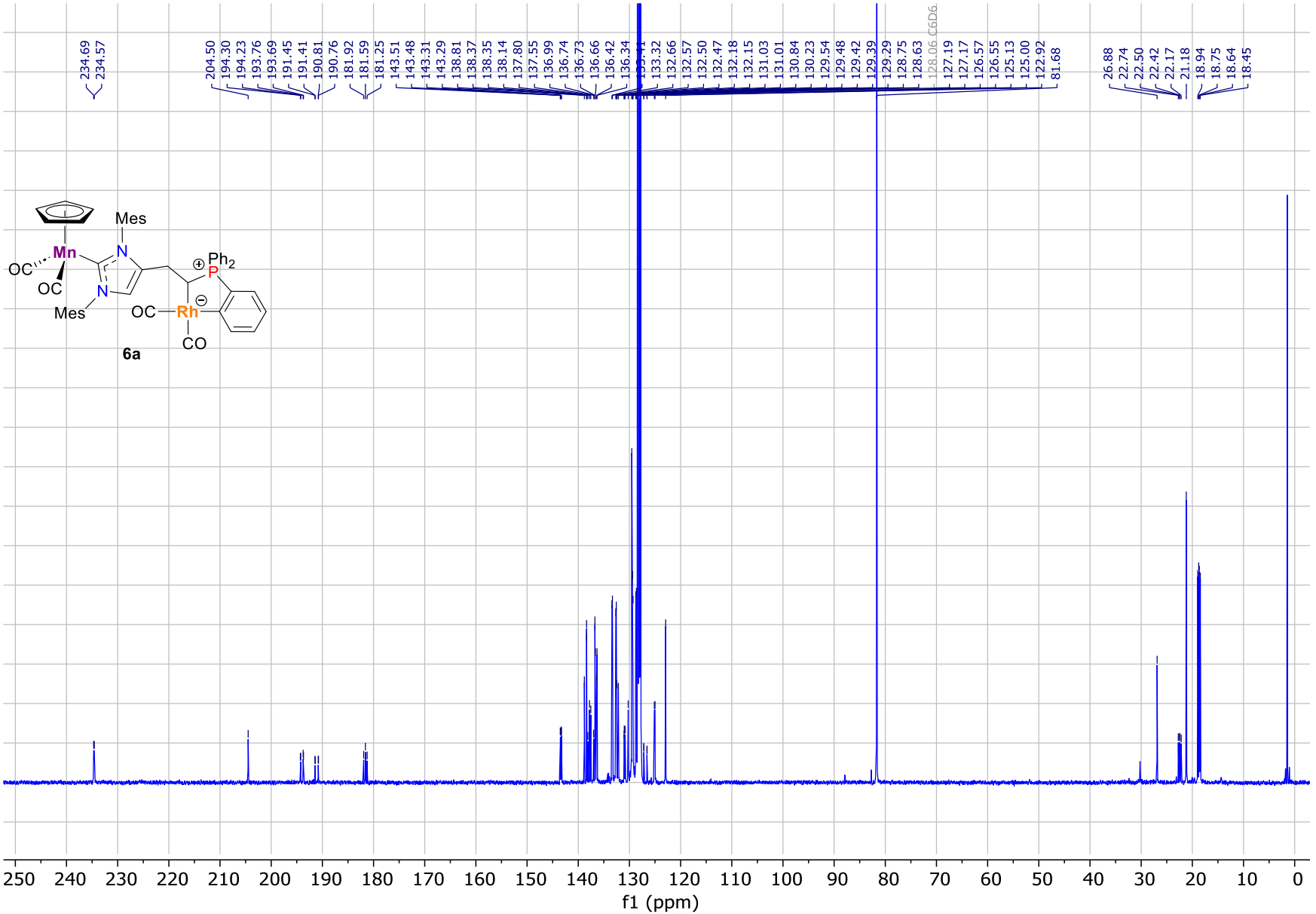


**Figure S22**. $^{13}C\{^{1}H\}$ NMR spectrum of complex **6a** (100.6 MHz, $C_6D_6$, 25°C).

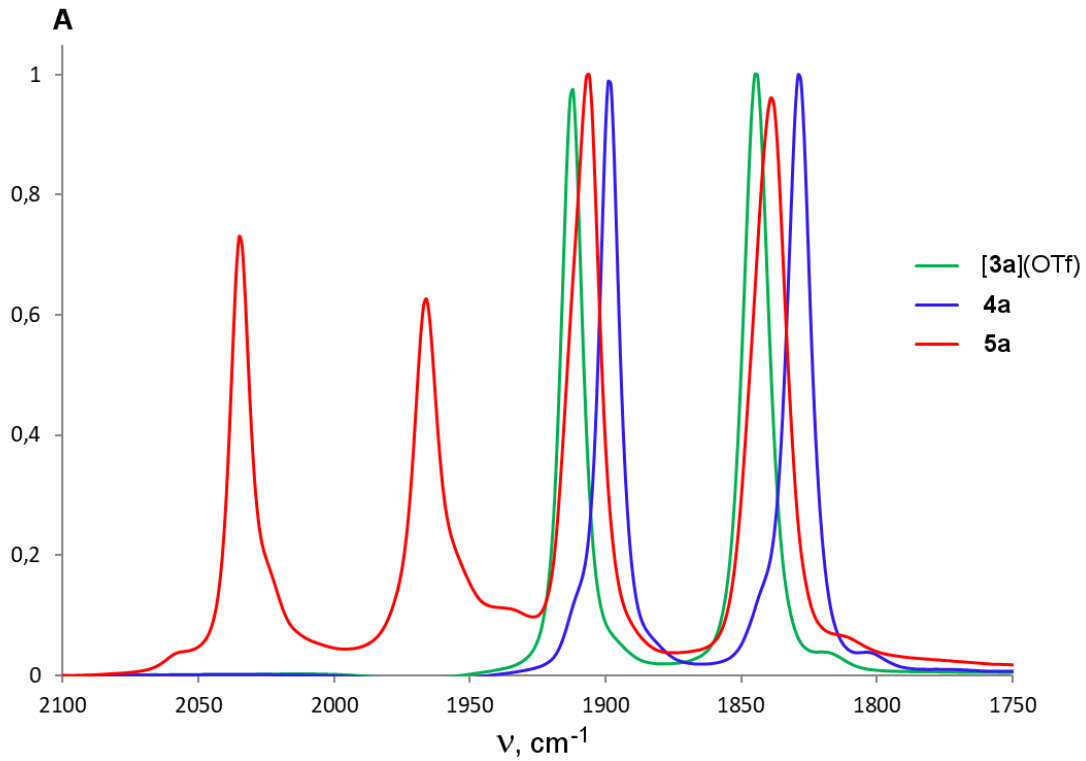


**Figure S23**. Superposition of normalized IR spectra (THF solution) for complexes [**3a**](OTf), **4a** and **5a**

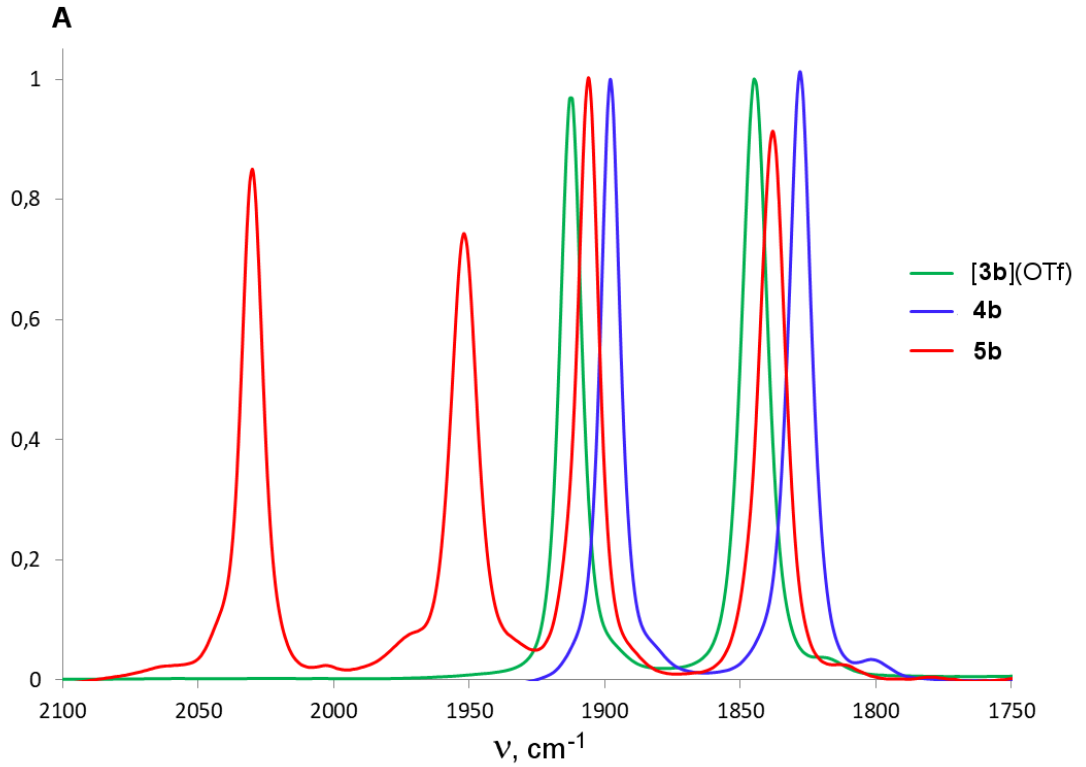


**Figure S24**. Superposition of normalized IR spectra (THF solution) for complexes [**3b**](OTf), **4b** and **5b**

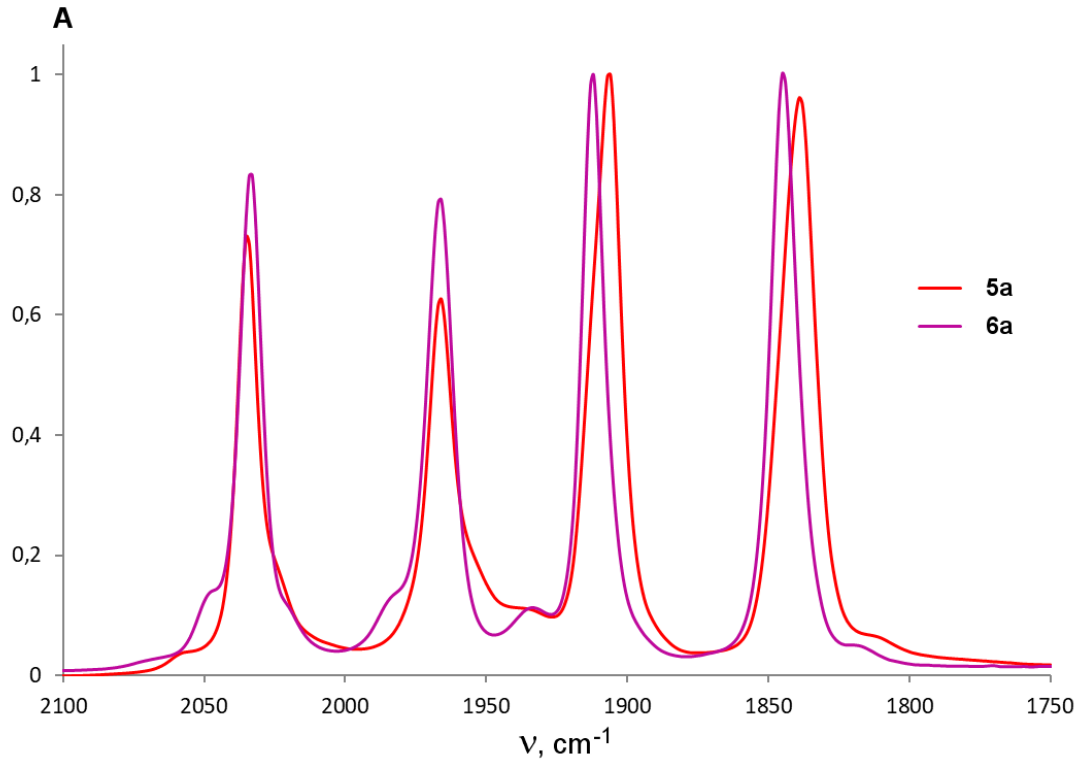


**Figure S25**. Superposition of normalized IR spectra (THF solution) for complexes **5a** and **6a**

## References


1. A. A. Grineva, D. A. Valyaev, V. César, O. A. Filippov, V. N. Khrustalev, S. E. Nefedov and N. Lugan, *Angew. Chem. Int. Ed.,* 2018, **57**, 7986.
2. M. C. Burla, R. Caliandro, B. Carrozzini, G. L. Cascarano, C. Cuocci, C. Giacovazzo, M. Mallamo, A. Mazzone and G. Polidori, *J. Appl. Cryst.,* 2015, **48**, 306.
3. G. M. Sheldrick, *Acta Cryst*., 2015, **A71**, 3.
4. L. J. Farrugia, *J. Appl. Crystallogr.*, 2012, **45**, 849.
5. R. H. Blessing, *Acta Cryst*., 1995, **A51**, 33.
6. A. L. Spek, *Acta Cryst.* 2015, **C71**, 9.
7. M. J. Frisch, G. W. Trucks, H. B. Schlegel, G. E. Scuseria, M. A. Rob, J. R. Cheeseman, J. A. M. Jr., T. Vreven, K. N. Kudin, J. C. Burant, J. M. Millam, S. S. Iyengar, J. Tomasi, V. Barone, B. Mennucci, M. Cossi, G. Scalmani, N. Rega, G. A. Petersson, H. Nakatsuji, M. Hada, M. Ehara, K. Toyota, R. Fukuda, J. Hasegawa, M. Ishida, T. Nakajima, Y. Honda, O. Kitao, H. Nakai, M. Klene, X. Li, J. E. Knox, H. P. Hratchian, J. B. Cross, V. Bakken, C. Adamo, J. Jaramillo, R. Gomperts, R. E. Stratmann, O. Yazyev, A. J. Austin, R. Cammi, C. Pomelli, J. W. Ochterski, P. Y. Ayala, K. Morokuma, G. A. Voth, P. Salvador, J. J. Dannenberg, V. G. Zakrzewski, S. Dapprich, A. D. Daniels, M. C. Strain, O. Farkas, D. K. Malick, A. D. Rabuck, K. Raghavachari, J. B. Foresman, J. V. Ortiz, Q. Cui, A. G. Baboul, S. Clifford, J. Cioslowski, B. B. Stefanov, G. Liu, A. Liashenko, P. Piskorz, I. Komaromi, R. L. Martin, D. J. Fox, T. Keith, M. A. Al-Laham, C. Y. Peng, A. Nanayakkara, M. Challacombe, P. M. W. Gill, B. Johnson, W. Chen, M. W. Wong, C. Gonzalez and J. A. Pople, *Gaussian, Inc.*, Wallingford, CT, 2009.
8. J.-D. Chai and M. Head-Gordon, *Phys. Chem. Chem. Phys.*, 2008, **10**, 6615.
9. (*a*) F. Weigend and R. Ahlrichs, *Phys. Chem. Chem. Phys.,* 2005, **7**, 3297; (*b*) F. Weigend, *Phys. Chem. Chem. Phys.,* 2006, **8**, 1057.
10. D. Andrae, U. Häußermann, M. Dolg, H. Stoll and H. Preuß, *Theor. Chim. Acta*, 1990, **77**, 123.
11. A. V. Marenich, C. J. Cramer and D. G. Truhlar, *J. Phys. Chem. B*, 2009, **113**, 6378.
12. M. P. Mitoraj, A. Michalaka and T. Ziegler, *J. Chem. Theory Comput.*, 2009, **5**, 962.
13. (*a*) F. Neese, *WIREs Comput. Mol. Sci.*, 2022, **12**, e1610; (*b*) F. Neese, *WIREs Comput. Mol. Sci.*, 2011, **2**, 73.
14. Chemcraft - graphical software for visualization of quantum chemistry computations. Version 1.8, https://www.chemcraftprog.com).
15. AIMAll (Version 19.10.12), T. A. Keith, TK Gristmill Software, Overland Park KS, USA, 2019 (https://www.aim.tkgristmill.com)
16. T. Lu and F. Chen, *J. Comput. Chem.*, 2012, **33**, 580.
17. NBO 6.0. E. D. Glendening, J. K. Badenhoop, A. E. Reed, J. E. Carpenter, J. A. Bohmann, C. M. Morales, C. R. Landis and F. Weinhold (Theoretical Chemistry Institute, University of Wisconsin, Madison, WI, 2013); http://nbo6.chem.wisc.edu/
18. A. A. Grineva, O. A. Filippov, Y. Canac, J. B. Sortais, S. E. Nefedov, N. Lugan, V. César and D. A. Valyaev, *Inorg. Chem*., 2021, **60**, 4015.